Molecular Biology of the Cell
Vol. 13, 2607–2625, August 2002

Scd5p and Clathrin Function Are Important for Cortical Actin Organization, Endocytosis, and Localization of Sla2p in Yeast

Kenneth R. Henry,*† Kathleen D'Hondt,‡§ JiSuk Chang,* Thomas Newpher,* Kristen Huang,*¶ R. Tod Hudson,* Howard Riezman,# and Sandra K. Lemmon*‖

*Department of Molecular Biology and Microbiology and †Program in Genetics, Case Western Reserve University, Cleveland Ohio 44106; and ‡Biozentrum of the University of Basel, CH-4056 Basel, Switzerland

Submitted January 8, 2002; Revised April 15, 2002; Accepted May 15, 2002
Monitoring Editor: Chris Kaiser

SCD5 was identified as a multicopy suppressor of clathrin HC-deficient yeast. *SCD5* is essential, but an *scd5*-Δ*338* mutant, expressing Scd5p with a C-terminal truncation of 338 amino acids, is temperature sensitive for growth. Further studies here demonstrate that *scd5*-Δ*338* affects receptor-mediated and fluid-phase endocytosis and normal actin organization. The *scd5*-Δ*338* mutant contains larger and depolarized cortical actin patches and a prevalence of G-actin bars. *scd5*-Δ*338* also displays synthetic negative genetic interactions with mutations in several other proteins important for cortical actin organization and endocytosis. Moreover, Scd5p colocalizes with cortical actin. Analysis has revealed that clathrin-deficient yeast also have a major defect in cortical actin organization and accumulate G-actin. Overexpression of *SCD5* partially suppresses the actin defect of clathrin mutants, whereas combining *scd5*-Δ*338* with a clathrin mutation exacerbates the actin and endocytic phenotypes. Both Scd5p and yeast clathrin physically associate with Sla2p, a homologue of the mammalian huntingtin interacting protein HIP1 and the related HIP1R. Furthermore, Sla2p localization at the cell cortex is dependent on Scd5p and clathrin function. Therefore, Scd5p and clathrin are important for actin organization and endocytosis, and Sla2p may provide a critical link between clathrin and the actin cytoskeleton in yeast, similar to HIP1(R) in animal cells.

INTRODUCTION

A major pathway for endocytosis involves the coat protein clathrin, comprised of heavy and light chains (HC and LC) and a large number of accessory factors. These proteins facilitate cargo capture, assembly of the clathrin lattice, membrane invagination, pinching off, and then uncoating of the vesicle once detached from the membrane. Many of these accessory proteins are held together by the cooperative interaction of different binding domains and appear to form a web beneath the cell surface (D'Hondt *et al.*, 2000; Brodsky *et al.*, 2001), although the role of the majority of these components and how they are regulated is still not completely understood.

Saccharomyces cerevisiae also contains clathrin HC and LC (Chc1p and Clc1p); however, there is only a partial dependence on clathrin for uptake at the cell surface (Payne *et al.*, 1988; Tan *et al.*, 1993; Huang *et al.*, 1997). On the other hand, the actin cytoskeleton appears to be essential for endocytosis in yeast, as genetic screens to identify factors involved in internalization have repeatedly uncovered proteins important for function of the cortical actin cytoskeleton (for reviews see Baggett and Wendland, 2001; D'Hondt *et al.*, 2000). Interestingly, many of these factors, or proteins that interact with these factors, are related to molecules that function in clathrin-mediated endocytosis in animal cells. For example, cortical actin patch components Rvs161p and Rvs167p are related to amphiphysins, which bind to clathrin HC, the heterotetrameric adaptor AP-2, and other regulatory components involved in clathrin-coated vesicle (CCV) formation in animal cells (David *et al.*, 1996; McPherson *et al.*, 1996; Ramjaun and McPherson, 1998; Slepnev *et al.*, 2000). Eps15-

Article published online ahead of print. Mol. Biol. Cell 10.1091/mbc.E02–01–0012. Article and publication date are at www.molbiolcell.org/cgi/doi/10.1091/mbc.E02–01–0012.

‖ Corresponding author. E-mail address: skl@po.cwru.edu.
Present addresses: § Department Biochemistry, University Ghent, Baertsoenkaai 3, B-9000 Ghent, Belgium; ¶ Department of Genetics, University of Pennsylvania, Philadelphia, PA 19104.

homology (EH) domain proteins, Pan1p, End3p, and Ede1p were identified in screens for endocytosis mutants in yeast and found to be important for cortical actin structures (Raths *et al.*, 1993; Bénédetti *et al.*, 1994; Tang and Cai, 1996; Tang *et al.*, 1997; Wendland and Emr, 1998; Gagny *et al.*, 2000). Animal Eps15 has an AP-2 binding region and interacts with NPF motifs via the EH domain in proteins like epsin, which in turn has clathrin and AP-2 binding domains (Benmerah *et al.*, 1996; Di Fiore *et al.*, 1997; Iannolo *et al.*, 1997; Chen *et al.*, 1998; Drake *et al.*, 2000). Yeast Pan1p is in a complex with End3p and another cortical actin patch component, Sla1p and has recently been shown to activate Arp2/3 complexes (Tang *et al.*, 2000; Duncan *et al.*, 2001; Zeng *et al.*, 2001). This Pan1p function may couple actin polymerization to the endocytic machinery. Interestingly, Pan1p binds to NPF motifs in the yeast epsin-related proteins, Ent1/2p, and AP180/CALM-like proteins, Yap180p's, which are associated with cortical patches but also directly bind to clathrin HC in yeast (Wendland and Emr, 1998; Wendland *et al.*, 1999). AP180/CALM promote the assembly of clathrin lattices in vitro and bind AP-2, and functional studies indicate that these proteins are also important components of the endocytic machinery in animal cells (McMahon, 1999; Traub *et al.*, 1999).

A role for cortical actin in endocytosis in animal cells has been less clear, because actin-depolymerizing drugs, e.g., latrunculin A (Lat-A), disrupt clathrin-mediated endocytosis in some cell types or under some growth conditions but not in others (Fujimoto *et al.*, 2000; Qualmann *et al.*, 2000; Apodaca, 2001). Also, in some polarized epithelial cells such drug treatments inhibit internalization at the apical surface but not the basolateral membrane (Apodaca, 2001). Although actin may not be absolutely required for endocytosis in animal cells, other recent results support an important association of the actin cytoskeleton with clathrin-coated pits. Treatment of cells with Lat-A increases the lateral mobility of clathrin-coated pits at the cell surface, suggesting that cytoskeletal elements may localize the endocytic machinery to domains of the plasma membrane (Gaidarov *et al.*, 1999; Bennett *et al.*, 2001). In addition, a few proteins that associate with both the actin cytoskeleton and clathrin-coated pit components have been identified. Two of these factors, mAbp1p and HIP1/HIP1R, were first identified in yeast as actin-associated proteins Abp1 or Sla2p (also known as End4p) or in screens for endocytic mutants (Drubin *et al.*, 1990; Holtzman *et al.*, 1993; Raths *et al.*, 1993). mAbp1 has an actin-binding region and a SH3 domain that also interacts with dynamin, and overexpression of the SH3 domain inhibits receptor-mediated endocytosis in animal cells (Kessels *et al.*, 2001).

HIP1 was identified as a huntingtin interacting protein and is closely related to HIP1R (Kalchman *et al.*, 1997; Wanker *et al.*, 1997; Seki *et al.*, 1998; Engqvist-Goldstein *et al.*, 1999). These proteins, as well as Sla2p, contain an epsin N-terminal homology (ENTH) domain found in epsin and AP180/CALM, which may help to recruit these proteins to the plasma membrane by binding cell surface phosphoinositides (Ford *et al.*, 2001; Itoh *et al.*, 2001). The C terminus of the yeast and mammalian Sla2p-related proteins is homologous to the talin-like F-actin binding module (McCann and Craig, 1997). The central region of HIP1/HIP1R, which includes a coiled-coiled segment, has recently been shown to bind directly to clathrin and facilitates association with clathrin-coated pits (Engqvist-Goldstein *et al.*, 2001; Metzler *et al.*, 2001; Mishra *et al.*, 2001; Waelter *et al.*, 2001; Legendre-Guillemin *et al.*, 2002). Although yeast Sla2p binds actin, shows partial colocalization with cortical actin patches, and is important for cortical actin organization and endocytosis (Holtzman *et al.*, 1993; Raths *et al.*, 1993; Wesp *et al.*, 1997), no connection to clathrin-mediated trafficking has been reported.

In previous studies we identified the *SCD5* gene as a multicopy suppressor of clathrin HC-deficient yeast (Nelson and Lemmon, 1993; Nelson *et al.*, 1996). Here we demonstrate that Scd5p is important for actin organization and endocytosis. This finding led us to examine actin localization in cells lacking clathrin. We find that similar to *scd5* mutants, loss of clathrin function causes major defects in cortical actin organization, and overexpression of *SCD5* partially suppresses this defect. Moreover, two-hybrid screening with the clathrin LC has identified Sla2p as an interacting protein. Scd5p also associates with Sla2p and Sla2p's cortical localization is dependent on both clathrin and Scd5p. These data suggest that clathrin and Scd5p may play a role in organizing or stabilizing the cortical actin network, which is important for endocytosis in yeast.

MATERIALS AND METHODS

Strains, Media, and Genetic Methods

Strains used in this study are listed in Table 1. YEPD (2% yeast extract, 1% peptone, and 2% dextrose), YEP-GAL (2% yeast extract, 1% peptone, and 2% galactose), 5-fluoro-orotic acid (FOA) plates, and synthetic complete dropout media (e.g., complete-uracil [C-URA]) were prepared as described in Nelson and Lemmon (1993). Yeast mating, sporulation, and tetrad analysis were performed as described (Guthrie and Fink, 1991). Yeast were transformed using the method of Gietz *et al.* (1995).

Plasmids

Plasmids were propagated in *Escherichia coli* DH5α. Important plasmids used in this study are listed in Table 2. A clone containing the *scd5-Δ338* truncation mutation under its own promoter was generated in two steps. A 4.6-kb *Bam*HI-*Cla*I *SCD5* fragment was cloned into pBluescript SK$^+$ (Stratagene, La Jolla, CA). This plasmid was subjected to site directed mutagenesis by the dut$^-$ ung$^-$ method (Kunkel *et al.*, 1987; McClary *et al.*, 1989) to generate pAC8. The primer 5′- GAGGAAGAGTAATTTACTAAGAATTCAG-3′ used for mutagenesis created two stop codons at positions 535 and 536 of the Scd5p coding sequence. The mutation was verified by DNA sequencing. pAC10 was made by cloning the *scd5-Δ338 Bam*HI-*Cla*I fragment from pAC8 into YIp5 (Botstein *et al.*, 1979). pJSC3 was generated by gap repair and contains *scd5-Δ338* from pAC8 in pRS315 (Sikorski and Hieter, 1989). The *GFP-SCD5* construct contains *SCD5* with the coding sequence for green fluorescent protein (GFP) fused in frame between codons 80 and 81 at a unique *Sac*I site. A PCR product for gap repair was made using primers 5′-CAGAAATAATCACTCAAATACAGCAGCTGATAATGCCACTAACGTGAGCTCTGGTGCTGGTGCTGGTGCTGC-3′ and 5′-CAGAAAGTGTTCGTACCTCCCCATTAGGTGGATTATCCTTTGAGGAGAGCTCACTTTGTACAATTCATCCATACC-3′ and a modified YGFP3 coding sequence as a template. The modified YGFP3 contains the coding sequences for an N-terminal 5 × GlyAla linker followed by yeast enhanced GFP-S65G, S72A (gift of C. Schaerer-Brodbeck). The PCR product was cotransformed into SL1462 with YEp24-*SCD5,* which was cut with *Sac*I. The final *CEN, LEU2, GFP-SCD5* plasmid, pKRH21, was made by gap repairing a

Table 1. *Saccharomyces cerevisiae* strains

Strain	Genotype	Source[a]
BWY236	*MAT*a *pan1-20 his3-Δ200 leu2-3,112 lys2-801 suc2-Δ9 trp1-Δ901 ura3-52*	1
DDY75	*MAT*a *abp1Δ::URA3 his4-619 lys2-801 ura3*	2
DDY301	*MATα sla1Δ::URA3 his4-619 leu2-3,112 lys2-801 ura3-52*	2
DDY771	*MATα sac6Δ::URA3 his4-619 ura3-52*	2
DDY951	*MATα srv2Δ::HIS3 his3-Δ200 leu2-3,112 lys2-801 ura3-52*	2
MY4495	*MATα rvs161Δ::LEU2 his3-Δ200 leu2 lys2-801 ura3-52*	3
SL13	*MATα chc1Δ::LEU2 leu2 scd1-v trp1 ura3-52* YCp50-*CHC1* [*CEN, URA3, CHC1*]	4
SL554	*MAT*a/*MATα GAL1::CHC1/GAL1::CHC1 ade6/+ his1/+ leu2/leu2 scd1-v/scd1-i trp1/trp1 ura3-52/ura3-52*	4
SL1462	*MAT*a *his3-Δ200 leu2 scd1-v trp1 ura3-52*	4
SL1528	*MAT*a/*MATα his3-Δ200/his3-Δ200 leu2/leu2 trp1/trp1 ura3-52/ura3-52 scd1-v/scd1-v*	4
SL1556	*MAT*a *sla2-41 (end4-1) bar1-1 his4 leu2 ura3*	5
SL1637	*MATα clc1Δ::HIS3 his3-Δ200 leu2 scd1-v trp1 ura3-52* pRS424-*CLC1* [2μ, *TRP1, CLC1*]	4
SL2726	*MATα chc1-521 his3-Δ200 leu2 scd1-v trp1 ura3-52*	
SL3004	*MATα ade2-101 gal4 gal80 his3 leu2 lys2-801 trp1-901 ura3-52*	
SL3416	*MATα yap1801Δ::URA3 his3-Δ200 leu2 scd1-v trp1 ura3-52*	4
SL3423	*MAT*a *yap1802Δ::KMX bar1-1 his3-Δ200 leu2 ura3-52*	4
SL3429	*MAT*a *yap1801Δ::URA3 yap1802Δ::KMX bar1-1 his3-Δ200 leu2 ura3-52*	4
SL3519	*MATα scd5-Δ338 gal2 his1 leu2 scd1-i trp1 ura3-52*	
SL3521	*MAT*a *scd5-Δ338 gal2 his1 leu2 scd1-i trp1 ura3-52*	
SL3593	*MAT*a *chc1Δ::LEU2 bar1-1 leu2 trp1 ura3-52*	
SL3739	*MAT*a *scd5-Δ338 gal2 his3-Δ200 leu2 trp1 ura3-52*	
SL3740	*MATα scd5-Δ338 gal2 his3-Δ200 leu2 trp1 ura3-52*	
SL3849	*MAT*a *rvs167Δ::TRP1 scd5-Δ338 His-(his1 and/or his4) leu2 trp1Δ::URA3 ura3-52*	
SL3855	*MATα rvs161Δ::LEU2 scd5-Δ338 his3-Δ200 leu2 ura3-52*	
SL3863	*MATα scd5-Δ338 srv2Δ::HIS3 his3-Δ200 leu2 ura3-52*	
SL3898	*MATα sac6Δ::URA3 scd5-Δ338* His- (*his4 and/or his3*) *ura3-52*	
SL3908	*MAT*a *abp1Δ::URA3 scd5-Δ338 his3-Δ200 his4-619 leu2 lys2-801 ura3*	
SL3920	*MAT*a/*MATα scd5-Δ338/scd5-Δ338 his3-Δ200/his3-Δ200 leu2/leu2 trp1/trp1 ura3-52/ura3-52*	
SL3921	*MAT*a *scd5Δ::TRP1 bar1-1 leu2 trp1 ura3-52* pCC545 [*CEN, LEU2, SCD5*]	
SL3993	*MAT*a *scd5Δ::TRP1 bar1-1 leu2 trp1 ura3-52* pJSC3 [*CEN, LEU2, scd5-Δ338*]	
SL4001	*MAT*a *ent1Δ::LEU2 his3-Δ200 leu2 lys2-801 trp1 ura3-52*	5
SL4002	*MATα ent2Δ::HIS3 his3-Δ200 leu2 suc2-Δ9 trp1 ura3-52*	
SL4049	*MAT*a *sla2-41(end4-1) his3-Δ200 leu2 trp1 ura3-52*	
SL4091	*MAT*a *ent1Δ::LEU2 scd5-Δ338 his3-Δ200 leu2 trp1 ura3-52*	
SL4097	*MAT*a *ent2Δ::HIS3 scd5-Δ338 his3-Δ200 leu2 trp1 ura3-52*	
SL4101	*MATα scd5-Δ338 yap1801Δ::URA3 his3-Δ200 leu2 trp1 ura3-52*	
SL4105	*MAT*a *scd5-Δ338 yap1802Δ::KMX his3-Δ200 leu2 trp1 ura3-52*	
SL4117	*MAT*a/*MATα end3Δ::HIS3-MX/+ scd5-Δ338/+ his3-Δ200/his3-Δ200 leu2/leu2 trp1/+ ura3-52/ura3-52*	
SL4162	*MAT*a *sla2-Δ::LEU2 bar1-1 his3-Δ200 leu2 lys2 ura3-52*	
SL4173	*MAT*a *chc1-521 sla2-41(end4-1) his3-Δ200 leu2 trp1 ura3-52*	
SL4182	*MAT*a *scd5-Δ338 his3-Δ200 leu2 scd1-v trp1 ura3-52*	
SL4212	*MAT*a *scd5-Δ338 yap1801Δ::URA3 yap1802Δ::KMX bar1-1 his3-Δ200 leu2 ura3-52*	
SL4260	*MAT*a *chc1-521 sla2-Δ::LEU2 bar1-1 his3-Δ200 leu2 ura3-52*	
SL4292	*MAT*a *clc1-Δ::HIS3 sla2-41(end4-1) his3-Δ200 leu2 trp1 ura3-52*	
SL4300	*MAT*a/*MATα scd5Δ::TRP1/scd5Δ::TRP1 his3-Δ200/his3-Δ200 leu2/leu2 trp1/trp1 ura3-52/ura3-52* pKRH21 [*CEN, LEU2, GFP-SCD5*]	
SL4301	*MAT*a/*MATα scd5Δ::TRP1/scd5Δ::TRP1 his3-Δ200/his3-Δ200 leu2/leu2 trp1/trp1 ura3-52/ura3-52* pJSC3 [*CEN, LEU2, scd5-Δ338*]	
SL4302	*MAT*a/*MATα scd5Δ::TRP1/scd5Δ::TRP1 his3-Δ200/his3-Δ200 leu2/leu2 trp1/trp1 ura3-52/ura3-52* pCC545 [*CEN, LEU2, SCD5*]	
SL4304	*MATα chc1-521 scd5-Δ338 his3-Δ200 leu2 trp1 ura3-52*	
SL4340	*MAT*a *chc1-Δ::LEU2 sla2-41(end4-1) his3-Δ200 leu2 scd1-v trp1 ura3-52*	
RH2951	*MATα rvs167-Δ::TRP1 bar1-1 his4 leu2 trp1-Δ::URA3 ura3-52*	5
YPJ96-4	*MAT*a *ade2 gal4-Δ gal80-Δ GAL2-ADE2 his3-Δ200 leu2-3,112 LYS2::GAL1-HIS3 met2::GAL7-lacZ trp1-901 ura3-52*	6

[a] Strains were generated for this study except where indicated. Several strains were derived from crosses to strains from other sources (not indicated). 1, Beverly Wendland; 2, David Drubin; 3, Mark Rose; 4, S. Lemmon (generated for previous studies); 5, Howard Riezman; 6, Phillip James.

Table 2. Important plasmids used in this study

Name	Features	Description
p31-10	2μ, *LEU2, GAD-SLA2-292-968*	Two hybrid prey fusing codons 292–968 of *SLA2* to the GAL4 activation domain coding sequence.
p31-2	2μ, *LEU2, GAD-SLA2-292-520*	Two hybrid prey fusing codons 292–520 of *SLA2* to the GAL4 activation domain coding sequence.
pAC10	*URA3, scd5-Δ338*	*scd5-Δ338* cloned into YIp5.
pCC545	*CEN, LEU2, SCD5*	*SCD5* in pRS315 (from Clarence Chan).
pGAD	2μ, *LEU2, GAD*	Two hybrid prey for expression of the GAL4 activation domain under control of the *ADH1* promoter (James *et al.*, 1996).
pGBDU	2μ, *URA3, GBD*	Two hybrid bait for expression of the GAL4 DNA binding domain under control of the *ADH1* promoter (James *et al.*, 1996).
pJC4	*CEN, URA3, GFP:ABP1*	*GFP:ABP1* expression vector (from David Drubin).
pJSC3	*CEN, LEU2, scd5-Δ338*	*scd5-Δ338* in pRS315.
pKH19	2μ, *LEU2, GAD-CLC1*	Two hybrid prey fusing the *CLC1* ORF to the GAL4 activation domain coding sequence.
pKH24	2μ, *LEU2, GAD-CHC1-655-1653*	Two hybrid prey fusing codons 655–1653 of *CHC1* to the GAL4 activation domain coding sequence.
pKH31	2μ, *URA3, GBD-CLC1*	Two hybrid bait fusing the *CLC1* ORF to the *GAL4* DNA binding domain coding sequence.
pKH47	2μ, *URA3, GBD-SLA2-292-501*	Two hybrid bait fusing codons 292–501 of *SLA2* to the GAL4 DNA binding domain coding sequence.
pKRH20	2μ, *URA3, GBD-scd5-Δ645*	Two hybrid bait fusing codons 1–227 of *SCD5* to the GAL4 DNA binding domain coding sequence.
pKRH21	*CEN, LEU2, GFP-SCD5*	Vector for expression of GFP-tagged Scd5p.
pNT1	2μ, *URA3, GBD-scd5-Δ338*	Two hybrid bait fusing codons 1–534 of *SCD5* to the GAL4 DNA binding domain coding sequence.
YCp50-*CHC1*	*CEN, URA3, CHC1*	*CHC1* in YCp50 (Lemmon and Jones, 1987).
YEp24-*SCD5*	2μ, *URA3, SCD5*	*SCD5* in YEp24 (Nelson *et al.*, 1996).

2.2-kb fragment from YEp*GFP-SCD5* into pCC545 gapped with *Xba*I.

pKH19 was created by engineering a *CLC1* PCR product with a 5′ *Nco*I site at the *CLC1* start codon and a *Pvu*II site downstream of the stop codon using primers 5′-CCATGGCAGAGAAATTC-3′ and 5′-GCGCAGCTGATCATTTAAGCACCG-3′, respectively. This was transferred by subcloning into pAS2 (Harper *et al.*, 1993) to generate pKH15. The *CLC1* ORF in pKH15 was then subcloned as a *Nco*I-*Bam*HI fragment into pACT2 (Harper *et al.*, 1993) to yield pKH19. pKH24 was generated by cloning a 5.0-kb *Cla*I-*Sal*I fragment containing *CHC1* into the *Sma*I-*Xho*I sites of pACT2. This fused codons 655-1653 of *CHC1* to the *GAL4* activation domain (GAD) coding sequence. In pKH31, a *Bam*HI fragment containing the *CLC1* ORF was cloned into pGBDU-C3 (James *et al.*, 1996) to generate a full-length *CLC1* ORF fused in frame to the coding region of the *GAL4* binding domain (GBD). pGAD-*SLA2*-(292–520) (p31-2) and pGAD-*SLA2*-(292–968) (p31-10) were isolated from a two-hybrid screen using a LC bait (pKH31). pKH47 was generated by moving *SLA2*-(292–520) from p31-2 as an *Eco*RI-*Pst*I fragment into pGBDU-C2 (James *et al.*, 1996). To generate pKRH20, a 0.7-kb *SCD5* PCR product was made using primers 5′-CGGGATCCATGTCGTTTGATTG-GCTTA-3′and 5′-CGAGATCTACACCTCCTCG-3′. This produced a *Bam*HI site at the *SCD5* start codon and a stop at codon 227 followed by a *Bgl*II site. This product was cloned into pGBDU-C1 (James *et al.*, 1996) fusing *SCD5* codons 1–227 to the GBD coding region. pNT1 was made by cloning a *Xba*I-*Sal*I fragment containing the *scd5-Δ338* mutation into the *Xba*I-*Sal*I sites of pKRH20. This resulted in a construct coding for residues 1–534 of Scd5p fused to the GBD (*GBD-scd5-Δ338*).

scd5-Δ338 Integration and END3 Gene Deletion

To integrate the *scd5-Δ338* allele at the *SCD5* chromosomal locus, pAC10 (*URA3, scd5-Δ338*) was linearized by *Blp*I and transformed into *scd5Δ::TRP1/SCD5* strains, selecting on C-URA. YIp5-*scd5-Δ338* could integrate adjacent to *SCD5* or *scd5Δ::TRP1*. Several integrants strains were plated on FOA to select for recombinants that lost the vector and adjacent sequence. FOA^R colonies were then screened for the loss of *TRP1* by plating replica plating on C-TRP. The Trp^- candidates represented events where integration occurred adjacent to the null allele and recombination excised *scd5Δ::TRP1* retaining the *scd5-Δ338* allele. The *scd5-Δ338* mutation generates a new *Dde*I site. The integration of *scd5-Δ338* was confirmed by heteroduplex analysis (Cotton, 1992) and PCR analysis combined with restriction enzyme digestion using *Dde*I. Tetrads were dissected to generate haploid progeny (SL3519, SL3521, and SL4182). The *scd5-Δ338* segregants were temperature sensitive for growth and expressed the truncated protein, as expected.

To generate a null allele of *END3* the complete ORF was replaced by *HIS3-MX6* using a PCR-based one-step gene-replacement method. The disruption PCR fragment was created with primers 5′-AGTTAGTGGGTATTGGAAAGGCCGGTAAAGATAACAGGG-ATCTCTGAAAACGGATCCCCGGGTTAATTAA-3′ and 5′-AA-CAAACAGTAAATATTACACATTCATGTACATAAAATTAA TTATCGGTGGAATTCGAGCTCGTTTAAAC-3′ using pFA6a-*HIS3MX6* (Wach, 1996) as the template. This PCR product was transformed into a *scd5-Δ338/SCD5* heterozygous diploid generating SL4117. Colony PCR was used to verify the disruption.

Two-hybrid Interaction Analysis

For the two-hybrid screen with *CLC1* as a bait, a yeast genomic two-hybrid library (James *et al.*, 1996) was transformed into SL3004. YPJ96-4A (James *et al.*, 1996) was transformed with pKH31 (pGBD-*CLC1*). The library strain and YPJ96-4A carrying pKH31 were mated in liquid culture for 4 h and plated on YEPD overnight. The cells were scraped from the plate and replated on synthetic medium lacking leucine, adenine, and uracil (C-ADE-LEU-URA) to select for mated zygotes and to monitor expression of the *GAL2-ADE2* reporter from YPJ96-4A. Colonies appeared after 3–5 d and were

further screened for false positives by testing against an empty bait vector and nonrelevant baits. Plasmids that passed these tests were sequenced from both ends of the insert.

Scd5p two-hybrid interactions studies used the mating method described above to generate strains expressing GAD and GBD plasmids. For clathrin two-hybrid interaction studies, YPJ96-4A was directly transformed with both GAD and GBD plasmids. For analysis of two-hybrid interactions, log phase cultures were diluted to 5×10^6 cells/ml, and equal volumes of cells were spotted on C-ADE-LEU-URA and C-LEU-URA plates. The plates were grown for 3–5 d at 30°C.

Other Assays

The alpha-factor endocytosis assay was performed as described previously (Dulic *et al.*, 1991). Lucifer yellow (LY) uptake was carried out by methods described in Munn *et al.* (1995). The latrunculin-A (Lat-A) halo sensitivity assay was performed as described by Ayscough *et al.* (1997), comparing a *scd5-Δ338* strain (SL4301) to an isogenic wild-type control (SL4302).

Microscopy

Yeast cells were grown to early exponential phase in YEPD or YEP-GAL. For F-actin, DNA, and chitin staining, cells were fixed with 3.7% formaldehyde and then stained with Alexa-568-phalloidin (Molecular Probes, Eugene, OR), 4′6′-diamidino-2-phenylindole (DAPI; Sigma, St. Louis, MO), or calcofluor white (Sigma), respectively, as described in Adams and Pringle (1991) and Pringle (1991). For simultaneous localization of GFP-Scd5p and actin, cells were fixed for 10 min with 2.0% formaldehyde and washed three times with PBS. The cells were stained with Alexa-594-phalloidin (Molecular Probes) as described in Adams and Pringle (1991) and visualized immediately. For GFP-Abp1p and actin colocalization, cells were fixed and processed as described in Heil-Chapdelaine *et al.* (1998).

For immunofluorescence, cells were prepared using a methanol/acetone fixation as described previously (Pringle *et al.*, 1991). Affinity-purified rabbit anti–C-terminal Sla2p antiserum (Yang *et al.*, 1999) was used at 1:75 dilution, and guinea pig anti-actin antiserum (Mulholland *et al.*, 1994) was used at 1:2000 dilution. For fluorescent visualization, FITC-conjugated goat anti-rabbit IgG and Alexa-594–conjugated goat anti-guinea pig IgG were used at 1:800 dilution.

Most of the microscopy was performed using a Zeiss Axioplan-2 microscope (Thornwood, NY) equipped with Nomarski differential interference contrast (DIC) optics, a plan-Neofluor 100× objective (numerical aperture 1.3), and a Hamamatsu C4742–95 cooled CCD camera (Bridgewater, NJ) using QED acquisition software. A LSM 410 confocal microscope equipped with a plan-Apochromat 100× objective (numerical aperture 1.4) was used for analysis of cells stained with Alexa-568-phalloidin in Figures 2 and 6. Images were manipulated in Adobe Photoshop (San Jose, CA).

For quantification of microscopy, 100–500 cells were counted for each condition. Cells were scored as having depolarized actin patches if there were ≥10 patches in the mother cell of cells with buds. Actin patches were scored "large" (or aggregates of actin) if they were ≥0.5 μm diameter. Normal patches seen in wild-type cells were typically 0.1–0.2 μm diameter. Large patches were usually delocalized to the mother cell, but each was counted as a single patch. G-actin "bars" were scored by their unusual stick-like or bar morphology and were only detected with anti-actin antibodies. Actin bar structures were never observed in wild-type cells.

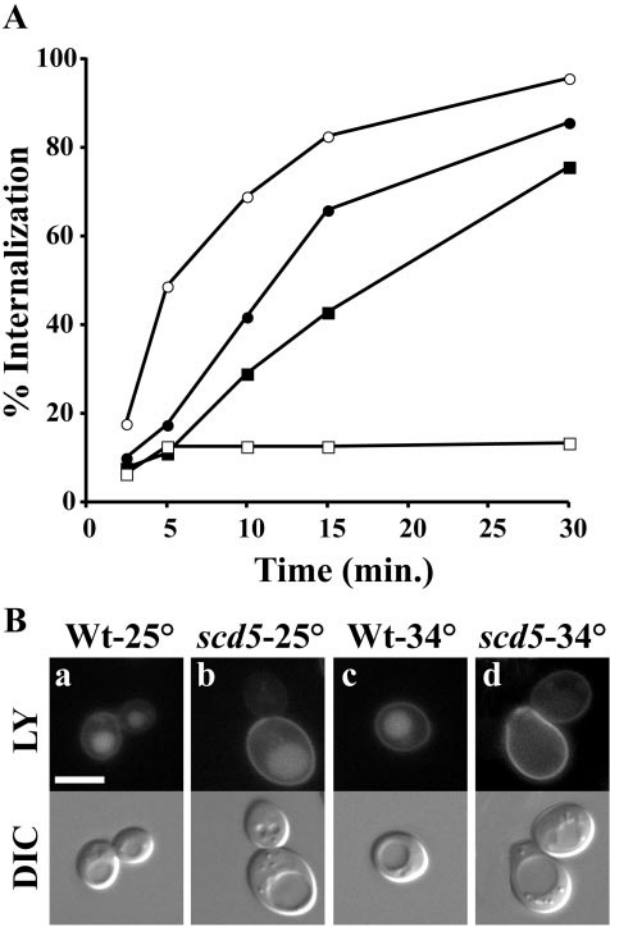

Figure 1. Endocytosis is defective in *scd5-Δ338* cells at 37°C. (A) Receptor-mediated internalization of radiolabeled α-factor. Cultures were grown at 25°C to mid log phase in YEPD, pelleted, and resuspended at 1×10^9 cells/ml in fresh YEPD. Cells were preincubated at 25 (●, ■) or 37°C (○, □) for 15 min before addition of ^{35}S-radiolabeled α-factor. Samples were harvested at times indicated and processed for determination of internalized α-factor. Strains are isogenic wild-type (SL3921; ●, ○) and *scd5-Δ338* (SL3993; ■, □). (B) Lucifer yellow (LY) uptake. Wild-type (SL1462; a and c) and *scd5-Δ338* (SL3739; b and d) cells were incubated at 25°C (a and b) or preshifted to 37°C (c and d) for 15 min. Then LY was added, and incubation was continued for 60 min. Cells were photographed using DIC (to visualize the vacuole) and fluorescence microscopy. Bar, 5 μm.

RESULTS

Endocytosis Is Defective in a scd5 Truncation Mutant

SCD5 was originally isolated as a multicopy suppressor of the lethality of a clathrin HC-deficient strain (Nelson and Lemmon, 1993). Previously we studied a temperature-sensitive *scd5-Δ338* mutant, expressing a 338-amino acid COOH-terminal truncation of Scd5p (Nelson *et al.*, 1996). This strain exhibits a partial post-Golgi secretion defect at the nonpermissive temperature but no obvious defects in sorting/retention of trans-Golgi proteins typical of clath-

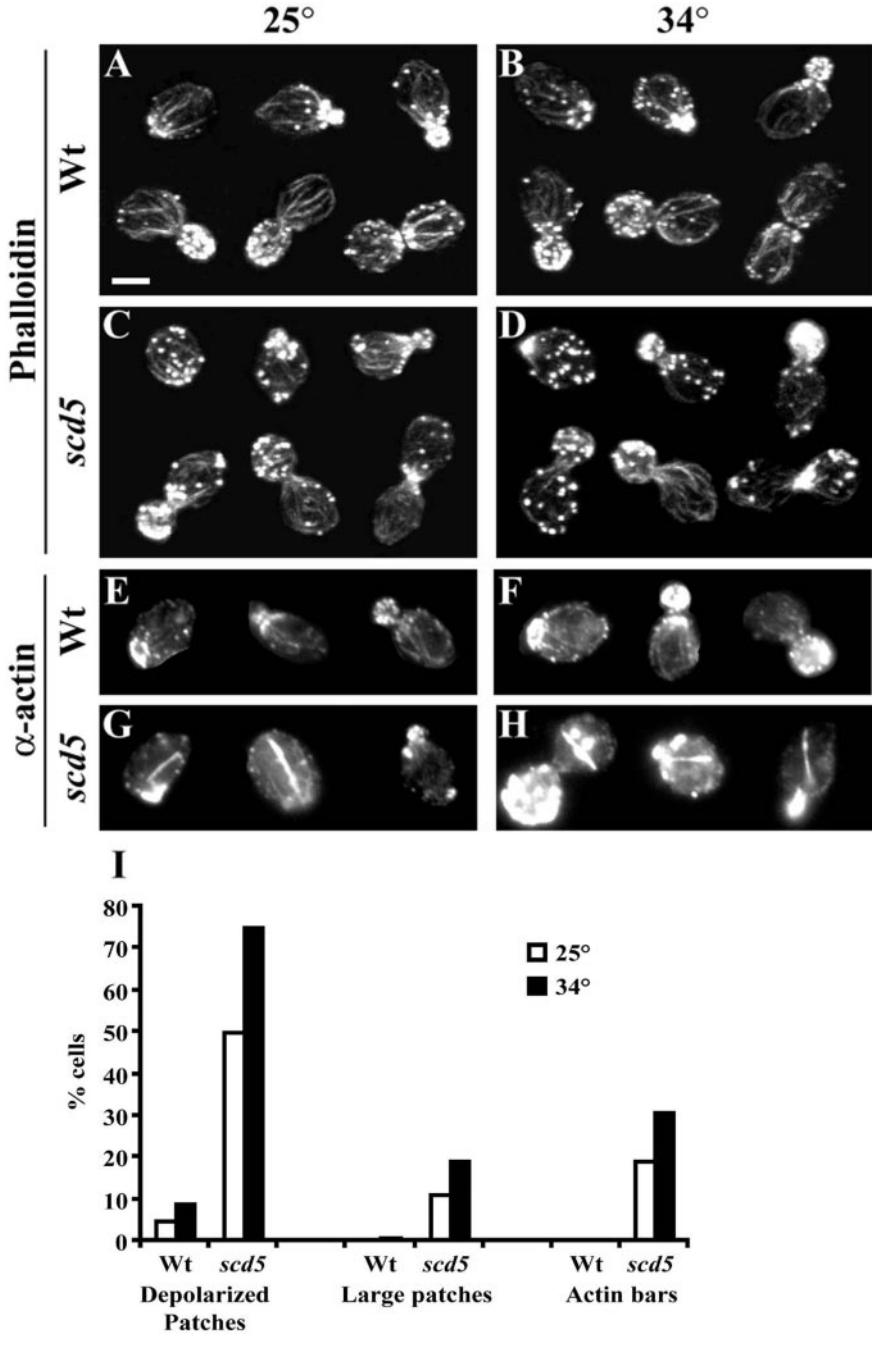

Figure 2. Actin organization is defective in *scd5*-Δ*338* cells. Wild-type (SL1528, A, B, E, and F) and *scd5*-Δ*338* (SL3920, C, D, G, and H) strains were grown on YEPD to log phase at 25°C. Cells were immediately harvested (A, C, E, and G) or shifted to 34°C (B, D, F, and H) for 3 h before fixation, staining, and microscopic visualization as described in MATERIALS AND METHODS (Bar, 5 μm). (A–D) Stained with Alexa-568-phalloidin to visualize filamentous actin; (E–H) indirect immunofluorescence with anti-actin antibodies. Examples of cells through the cell cycle are shown in A–D. (I) Bar graph showing percent of cells with depolarized patches, large patches, or actin bars from the same experiments as shown in A–H. Quantification was determined as described in MATERIALS AND METHODS.

rin mutants (Nelson *et al.*, 1996). Because clathrin mutants also display slowed receptor-mediated endocytosis (Payne *et al.*, 1988; Tan *et al.*, 1993; Huang *et al.*, 1997), we examined whether Scd5p function is required for internalization of α-factor by its receptor, Ste2p (Figure 1A). At 25°C, internalization of ^{35}S-labeled α-factor was nearly normal compared with an isogenic wild-type strain. Preshifting *scd5*-Δ*338* cells to 37°C for 15 min resulted in a rapid and complete block in internalization of α-factor.

We also examined fluid-phase endocytosis in the *scd5* mutant by visualizing accumulation of the fluorescent dye lucifer yellow (LY) in the vacuole (Figure 1B). At 25°C to 35–55% of *scd5*-Δ*338* cells, depending on the isolate, showed vacuolar staining with LY. When cells were shifted to 37°C, uptake to the vacuole was completely blocked. Nearly 100% of wild-type cells internalized LY at either temperature. We conclude that Scd5p is required for both fluid-phase and receptor-mediated endocytosis.

Scd5p Is Important for Actin Organization

The endocytic defects of *scd5-Δ338* are much more severe than observed in clathrin mutants (Payne *et al.*, 1988; Tan *et al.*, 1993; Huang *et al.*, 1997) but resemble the internalization phenotypes of a number of mutants with a perturbed cortical actin cytoskeleton (e.g., see Kübler and Riezman, 1993; Bénédetti *et al.*, 1994; Munn *et al.*, 1995; Wesp *et al.*, 1997; Madania *et al.*, 1999; Schaerer-Brodbeck and Riezman, 2000). Moreover, some of these mutants, e.g., *sla2/end4*, *rvs161*, *rvs167*, and *act1*, also display partial post-Golgi secretory defects similar to those of *scd5-Δ338* (Novick and Botstein, 1985; Nelson *et al.*, 1996; Mulholland *et al.*, 1997; Breton *et al.*, 2001). Therefore, we examined actin organization in the *scd5-Δ338* mutant.

Two major actin filament-based (F-actin) structures are seen in yeast cells: actin cables and cortical actin patches (Adams and Pringle, 1984; Pruyne and Bretscher, 2000a). The cables, which are bundles of actin filaments, are responsible for polarized growth and delivery of secretory vesicles, cell wall material, organelles, and other proteins into the growing daughter cell. Cortical actin patches appear at the site of bud emergence and then localize primarily to the growing bud. Late in the cell cycle, patches first redistribute across mother and daughter cells. Finally, cables reorient toward the mother/daughter cell neck and patches concentrate at the bud neck where they are involved in septum formation and cytokinesis (See Figure 2, A and B).

To examine actin organization, wild-type and *scd5-Δ338* cells were grown at 25°C or shifted to 34°C for 3 h and stained with Alexa-568-phalloidin to label F-actin. Many *scd5-Δ338* mutant cells displayed aberrant patch organization, which was more severe at 34°C (Figure 2, C and D). Often these patches were depolarized to the mother cell, and some patches appeared larger than normal cortical actin structures (see Figure 2I for quantification of patch morphology). In addition, there were fewer or thinner cables in some *scd5-Δ338* cells, particularly in those that had larger patches, and in some cells the cables seemed to be misoriented.

There is very little nonpolymerized globular actin (G-actin) and it is not aggregated in normal yeast cells; however, G-actin aggregates or actin bars are observed in the presence of some mutations affecting the actin cytoskeleton (e.g., *srv2Δ*, *act1-2*, or *sla1Δ*; Novick and Botstein, 1985; Holtzman *et al.*, 1993; Cope *et al.*, 1999). Therefore we stained *SCD5* and *scd5-Δ338* cells with anti-actin antibodies, which detect both F- and G-actin. The staining of wild-type cells resembled the phalloidin pattern (Figure 2, E and F). In contrast, many *scd5-Δ338* cells accumulated actin bars and other large aggregates of actin, presumably G-actin, that were not observed by phalloidin staining (examples shown in Figure 2, G and H, and quantification in I).

Latrunculin A (Lat-A) is an inhibitor of actin assembly, and many mutations affecting actin organization are hypersensitive to the drug (Ayscough *et al.*, 1997). In addition, *sla1Δ* and *end3Δ* are slightly resistant to Lat-A (Ayscough *et al.*, 1997). We found that *scd5-Δ338* also confers mild resistance to this inhibitor. In a Lat-A halo assay the *scd5-Δ338* mutant (SL4301) gave a diameter ratio of 0.8 ± 0.05 compared with an isogenic wild-type strain (SL4302; average of three experiments), although the observed effect could actually be stronger because *scd5-Δ338* grows slightly slower than wild type.

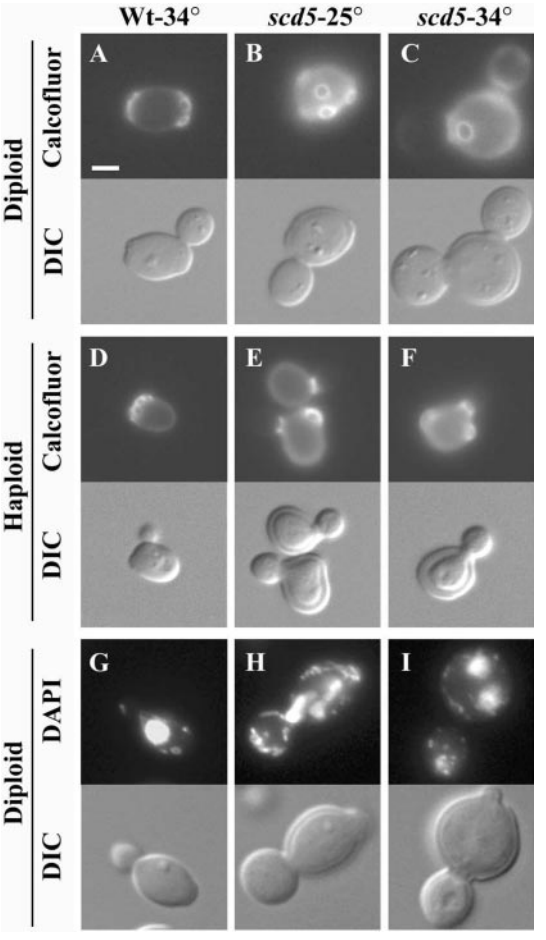

Figure 3. *scd5-Δ338* cells exhibit cell polarity defects. Cells were grown in YEPD to log phase at 25°C or shifted to 34°C for 3 h before fixation and visualization. Top panels: (A–F) calcofluor white staining of chitin; (G–I) cells stained with DAPI to visualize DNA. Bottom panels: DIC images. Strains are as follows: wild-type diploid (SL1528) at 34°C (A and G); *scd5-Δ338* diploid (SL3920) at 25 (B and H) or 34°C (C and I); wild-type haploid (SL1462) at 34°C (D); *scd5-Δ338* haploid (SL3739) at 25 (E) or 34°C (F). Bar, 5 μm.

The *scd5-Δ338* mutant was examined for other phenotypes that are often associated with perturbation of the actin cytoskeleton. Mutations affecting actin can cause defects in bud site pattern selection and depolarized chitin deposition (Novick and Botstein, 1985; Yang *et al.*, 1997). Also, multinucleated cells and aberrant morphologies, including multibudded cells, are sometimes seen because of the polarity defects in actin mutants (Novick and Botstein, 1985; Yang *et al.*, 1997). To examine budding pattern, cells were stained with calcofluor white, which labels chitin in bud scars left on mother cells after cytokinesis (Pringle, 1991). In the *scd5-Δ338* cells chitin was delocalized both at 25°C and after shift to 34°C for 3 h (Figure 3, B and C, and 3, E and F). Also, the majority of *scd5-Δ338* diploids (>75%) displayed random bud scar placement at 25 and 34°C, whereas >93% of wild-type cells showed the normal bipolar budding pattern (Figure 3, A–C). Haploid *scd5-Δ338* cells also showed random

Table 3. Genetic interactions between *scd5-Δ338* and mutations in other genes affecting endocytosis and/or actin cytoskeletal organization

Relevant genotype	Growth range[a]	Actin[b]
A. *WT*	25–37°C	Normal
scd5-Δ338	25–34°C	Depolarized cables and patches, fewer or thinner cables
B. Synthetic lethal		
end3Δ	25–34°C	ND[c]
endΔ scd5-Δ338	Lethal	ND
sla2-41	25–34°C	ND
sla2-41 scd5-Δ338	Lethal	ND
pan1-20	25–34°C	ND
pan1-20 scd5-Δ338	Lethal	ND
C. Strong negative interaction		
abp1Δ	25–37°C	Normal
abp1Δ scd5-Δ338	25°C	Depolarized cables and patches, fewer cables, larger patches
rvs161Δ	25–34°C	Depolarized cables and patches
rvs161Δ scd5-Δ338	25°C	Depolarized cables and patches, increased patches, fewer cables
rvs167Δ	25–34°C	Depolarized patches and cables
rvs167Δ scd5-Δ338	25°C	Depolarized patches and cables, increased patches, fewer cables
D. Weak negative interactions		
sac6Δ	25–34°C	Fewer cables, depolarized patches
sac6Δ scd5-Δ338	25–30°C	Depolarized cables and patches, fewer cables and larger patches
E. No observed interactions[d]		
ent1Δ, *ent2Δ*, *sla1Δ*, *srv2Δ*, *yap1801Δ*, *yap1802Δ*, *yap1801Δ yap1802Δ*		

[a] Strains were replica plated from patches or streaked onto YEPD plates and grown for 3 days at 25, 30, 32, 34, and 37°C. Note that the *scd5-Δ338* mutant grows very slowly at 34°C.

[b] Actin was visualized by staining with Alexa-phalloidin after growth at 25°C.

[c] ND, not determined.

[d] The *scd5-Δ338* mutation was not combined with *ent1Δ ent2Δ*, because the double *ent* mutant is inviable.

budding (72% at 34°C), rather than the normal axial budding pattern (Figure 3, E–F). Haploid and diploid mutants were heterogeneous in size and shape but were generally larger and rounder than wild-type cells (Figures 1 and 3). Cell surface rims were observed in DIC profiles of *scd5-Δ338* mutant cells, indicating the mutation results in thickened cell walls (Figure 3). EM analysis also showed thickening of the mother cell wall, similar to other cortical actin mutants. In addition, mutant cells (17 and 33% of diploids at 25 and 34°C, respectively) were often multibudded, mostly appearing to have a small aborted bud on the mother cell (see Figure 3I). Similar numbers were observed in haploids. The concentrated patches of F-actin sometimes found in mother cells (for example, see Figure 2C) were often positioned at these sites of aborted budding. A significant number of *scd5-Δ338* cells were multinucleated (up to 14% at 34°C), compared with <1% seen in wild-type cells (Figure 3, G and H). From these data we conclude that *scd5-Δ338* causes cell polarity defects typical of many mutations affecting the actin cytoskeleton.

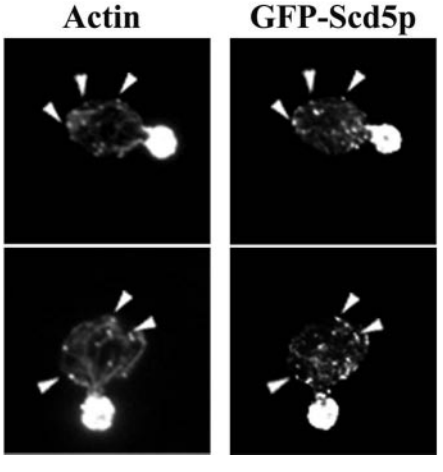

Figure 4. Scd5p localizes with cortical actin. SL4300 (*scd5Δ/scd5Δ* + pKRH21 [*CEN*, *LEU2*, *GFP-SCD5*]) was grown at 30°C to log phase. Cells were prepared for visualization of F-actin (left) and GFP-Scd5p (right) as described in MATERIALS AND METHODS. Arrows indicate examples of mother cell actin patches that also show GFP-Scd5p fluorescence.

scd5-Δ338 *Exhibits Genetic Interactions with Mutations in Genes Encoding Other Proteins that Modulate the Actin Cytoskeleton and/or Endocytosis*

Many mutations affecting actin cytoskeletal organization and/or endocytosis cause synergistic phenotypes when combined, and many of the normal gene products are physically associated or directly interact (Botstein *et al.*, 1997; D'Hondt *et al.*, 2000). Therefore, we examined genetic inter-

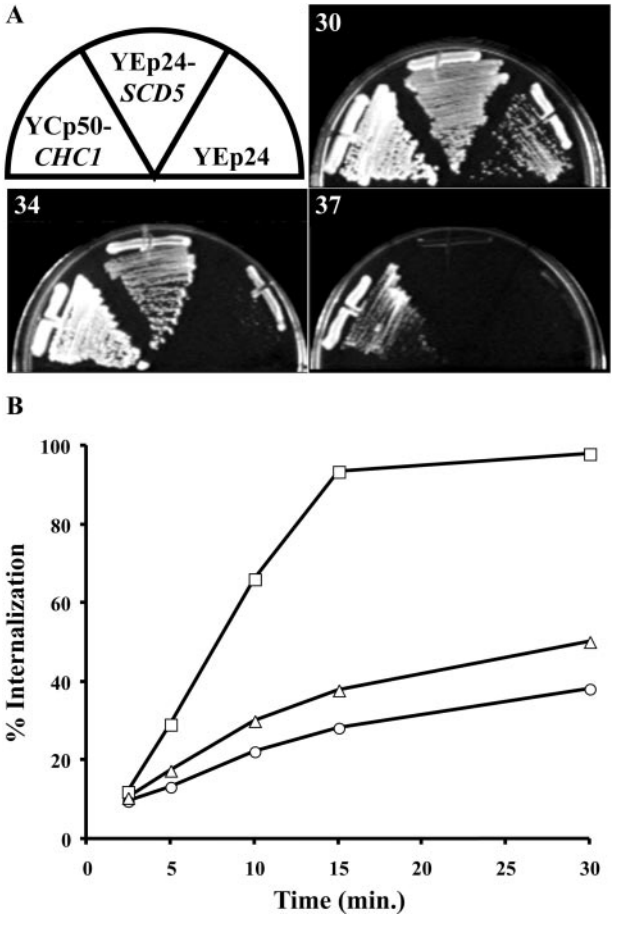

Figure 5. Overexpression of *SCD5* partially suppresses the temperature-sensitive growth phenotype, but not the endocytic defect of *chc1*Δ *scd1-v* cells. (A) A *chc1*Δ *scd1-v* strain (SL3593) transformed with YEp24, YEp24-*SCD5*, or YCp50-*CHC1* was streaked onto YEPD and incubated for 3 d at 30, 34, or 37°C. (B) Cells were grown to log phase in selective medium (C-URA). Radiolabeled α-factor was prebound to cells at 4°C in YEPD. Cells were pelleted, and then endocytosis was initiated by resuspending in prewarmed YEPD at 30°C. Samples were taken at the indicated times and cells were processed to determine percentage of α-factor internalized. Strains are *chc1*Δ *scd1-v* (SL3593) transformed with YEp24 (○), YEp24-*SCD5* (△) or YCp50-*CHC1* (□).

actions between *scd5*-Δ*338* and mutations in genes important for these processes (Table 3). Haploids carrying mutations in genes to be tested were crossed to *scd5*-Δ*338* and subjected to segregation analysis. Then wild-type, single, and combination mutant progeny from tetrads were analyzed for synthetic growth phenotypes. We found *sla2-41(end4-1)*, *pan1-20*, and *end3*Δ were synthetically lethal with *scd5*-Δ*338*. *abp1*Δ, and *rvs161*Δ, and *rvs167*Δ showed strong negative synergistic growth defects with *scd5*-Δ*338*, as the double mutants were inviable at 30°C and often grew very slowly at 25°C, whereas the single mutants grew relatively well or like wild-type cells at these temperatures. A weaker negative genetic interaction was observed with *sac6*Δ, where the *sac6*Δ *scd5*-Δ*338* double mutant grew at 30°C but not at 32°C. These genetic interactions are likely to be specific because *ent1*Δ, *ent2*Δ, *sla1*Δ, *srv2*Δ, *yap1801*Δ, *yap1802*Δ, and *yap1801*Δ *yap1802*Δ had no effect when combined with *scd5*-Δ*338*. In these cases, growth of the multiple mutants was similar to that of the *scd5*-Δ*338* mutant alone.

The double mutants were also analyzed for enhanced defects in actin cytoskeleton organization at 25°C, compared with the single mutants, by staining with Alexa-568-phalloidin (summarized in Table 3). Generally the results paralleled the growth phenotypes. The mutations that exacerbated the growth of *scd5*-Δ*338* the most caused more severe actin defects. For example *abp1*Δ *scd5*-Δ*338* double mutants had fewer cables and fewer, but larger and depolarized, patches than *scd5*-Δ*338* alone, even although the actin cytoskeleton in *abp1*Δ single mutants was normal at 25°C (Drubin *et al.*, 1990). In addition, disruptions in *RVS161* and *RVS167*, which exhibit some defects in the actin cytoskeleton on their own (Bauer *et al.*, 1993; Sivadon *et al.*, 1995), resulted in the appearance of more and depolarized patches and fewer actin cables than the single mutants. *sac6*Δ, which also perturbs actin (Adams *et al.*, 1991), resulted in the appearance of fewer cables and a few larger patches in combination with *scd5*-Δ*338*. This weaker synergistic effect on actin is consistent with the more limited effect of *sac6*Δ on growth of the *scd5* mutant. The *scd5*-Δ*338* double mutants that contained *sla1*Δ, *ent1*Δ, *ent2*Δ, *yap1801*Δ, *yap1802*Δ, or *srv2*Δ did not show an exaggerated actin phenotype. Instead, these double mutants resembled the *scd5*-Δ*338* mutant, despite the fact that some of these mutations (*sla1*Δ and *srv2*Δ; Vojtek *et al.*, 1991; Holtzman *et al.*, 1993; Lila and Drubin, 1997) cause actin phenotypes on their own. The noninteracting mutations also did not exacerbate the LY internalization defect of *scd5*-Δ*338* at 25°C. We note that most of the mutations causing enhanced growth and actin cytoskeleton phenotypes with *scd5*-Δ*338* also had major endocytic defects on their own, so the LY analysis was uninformative. Overall this analysis indicates that mutations in several genes affecting actin organization and endocytosis also genetically interact with *scd5*-Δ*338*, further supporting a role for Scd5p in actin function.

Scd5p Colocalizes with Cortical Actin

Because *scd5*-Δ*338* causes several phenotypes observed in other mutants with defects in cortical actin organization, we examined localization of Scd5p using a GFP-tagged protein in cells where this was the only source of the protein. The plasmid containing *GFP-SCD5* (pKRH21) complements *scd5*Δ completely. We found that GFP-Scd5p colocalized with cortical actin patches visualized with Alexa-594-phalloidin. This was most easily observed in budding cells, where there was a striking polarized distribution of Scd5p to the bud (Figure 4). GFP-Scd5p could also be seen in mother cell actin patches. However, there was not complete overlap of Scd5p and cortical patches, as has been observed for other actin patch proteins like Sla2p (Yang *et al.*, 1999). Overall, the localization results further support a role for Scd5p in cortical actin function.

Clathrin Deficiency Causes Defects in Cortical Actin Organization

Because Scd5p is important for endocytosis and the gene was isolated by its ability to rescue inviable strains of clath-

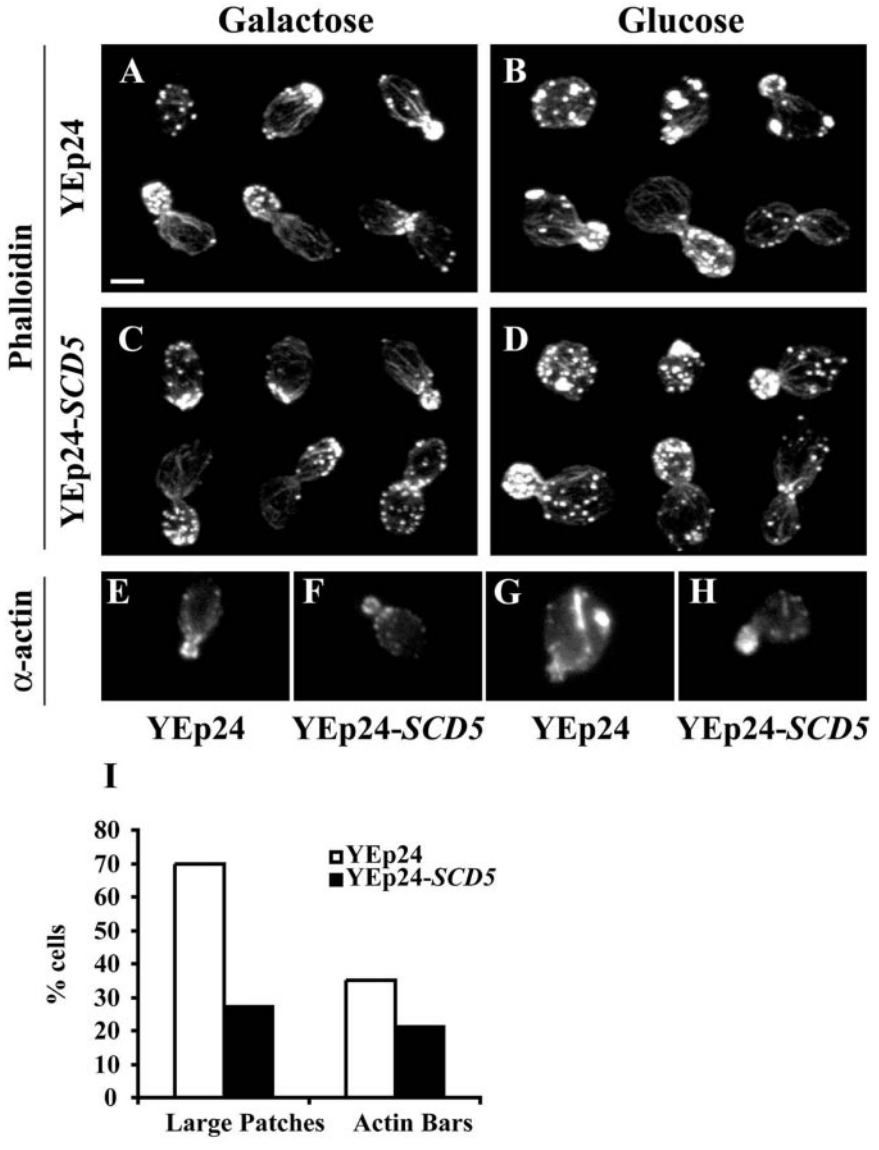

Figure 6. Overexpression of *SCD5* partially suppresses the actin organization defect of clathrin-deficient yeast. A *GAL1:: CHC1* strain (SL554) was transformed with YEp24 (A, B, E, and G) or YEp24-*SCD5* (C, D, F, and H). Precultures were grown on selective C-URA + 2% galactose. Then cells were washed and resuspended in medium containing galactose (A, C, E, and F) or glucose to deplete clathrin HC (B, D, G and H) for 15 h at 30°C. Cells were then fixed and stained with Alexa-568 phalloidin (A–D) or anti-actin antibodies (E–H). Bar, 5 μm. (I) Graph showing the percentage of cells from the above cultures with large patches or actin bars.

rin HC- (Chc1p) deficient yeast (Nelson and Lemmon, 1993; Nelson *et al.*, 1996), we considered the possibility that this interaction is associated with endocytic defects seen in viable clathrin mutants. To investigate this, we transformed a viable clathrin HC null strain with YEp24, YEp24-*SCD5,* or a *CHC1* complementing plasmid (YCp50-*CHC1*) and tested for suppression of the *chc1*Δ growth and receptor-mediated endocytosis defects. *SCD5* overexpression suppressed the temperature sensitivity of the viable *chc1*Δ strain quite well at 34°C, although not at 37°C (Figure 5A). However, the slowed α-factor internalization seen in *chc1*Δ mutants was minimally affected by overexpression of *SCD5* (Figure 5B), even at 30°C, a permissive growth temperature.

Because *scd5*-Δ*338* causes actin defects, we next examined whether clathrin deficiency affects actin organization. We made use of a strain expressing *CHC1* under control of the repressible *GAL1* promoter as its only source of clathrin HC. *GAL1::CHC1* cells grown in galactose medium showed the normal pattern of actin localization by phalloidin staining (Figure 6A). Shifting to glucose for 15 h, which completely depletes Chc1p (Nelson and Lemmon, 1993), caused accumulation of larger actin patches. These large patches were usually delocalized to the mother cell during bud growth and were observed in 70% of the cells (Figure 6, B and I). The clathrin-depleted cells also displayed fewer actin patches at the mother-daughter neck during cytokinesis, when compared with cells expressing clathrin HC (Figure 6B). Furthermore, 35% of HC-depleted cells contained actin bars, whereas none of the cells grown on galactose contained G-actin bars (Figure 6, E, G, and I). Similar actin phenotypes were seen in *chc1*Δ and clathrin LC-deficient (*clc1*Δ) strains.

We next tested whether overexpression of *SCD5* could suppress the actin organization defect of Chc1p-depleted cells. On

galactose medium *GAL1:CHC1* cells transformed with YEp-*SCD5* had normal actin organization (Figure 6, C and F), although during cytokinesis more depolarized patches were observed in the mother and daughter cells (see Figure 6C, 2nd row, 3rd cell). However, in total, <10% of cells with YEp*SCD5* had depolarized patches when grown on galactose, and no large patches or bars were observed (Figure 6F). On glucose medium the number of Chc$^-$ cells with large patches was significantly reduced by overexpression of *SCD5* (Figure 6, D and I). Thus, extra Scd5p prevented aggregation of cortical actin. However, these normal size patches were still delocalized in the majority (83%) of the clathrin-deficient cells (Figure 6D). The actin bar defect of the Chc$^-$ cells was also partially suppressed by increased Scd5p (Figure 6, H and I). In addition, *SCD5* overexpression partially suppressed the enlarged size and morphological defects observed in *chc1*Δ and *clc1*Δ mutants.

Genetic Interactions of scd5-Δ338 *and* chc1 *Mutations*

Because clathrin-deficient yeast have actin phenotypes and overexpression of *SCD5* partially rescues this defect, we examined whether mutations in *CHC1* and *SCD5* cause synthetic phenotypes. We made use of a *chc1-ts* mutant (*chc1-521*), which exhibits TGN sorting and endocytic defects at 37°C, but is normal at 25°C (Seeger and Payne, 1992a, 1992b; Tan *et al.*, 1993). The *chc1-ts* mutant was crossed to a *scd5-Δ338* strain, and haploid progeny from tetrad dissection were analyzed. We found that although both the *chc1-ts* and *scd5-Δ338* spore progeny grew up to 32 or 34°C, the *chc1-ts scd5-Δ338* double mutants grew very poorly at 25°C and were completely inviable at 30°C or higher (Figure 7A). Also, fluid-phase endocytosis of LY in the double mutant was almost completely blocked at 25°C (only 7% of cells had vacuolar staining), although 98% of the *chc1-ts* and 39% of the *scd5-Δ338* single mutants internalized the dye at this temperature (Figure 7B). Furthermore, although the *chc1-ts* mutant showed no actin phenotype at 25°C, it exacerbated the *scd5-Δ338* cortical actin defect causing appearance of more and larger actin patches than were observed in the *scd5* mutant alone (Figure 7C). There were no large patches in the *chc1-ts* mutant and <10% of *scd5-Δ338* mutant had large patches, whereas 50% of the double mutant cells contained large patches of F-actin.

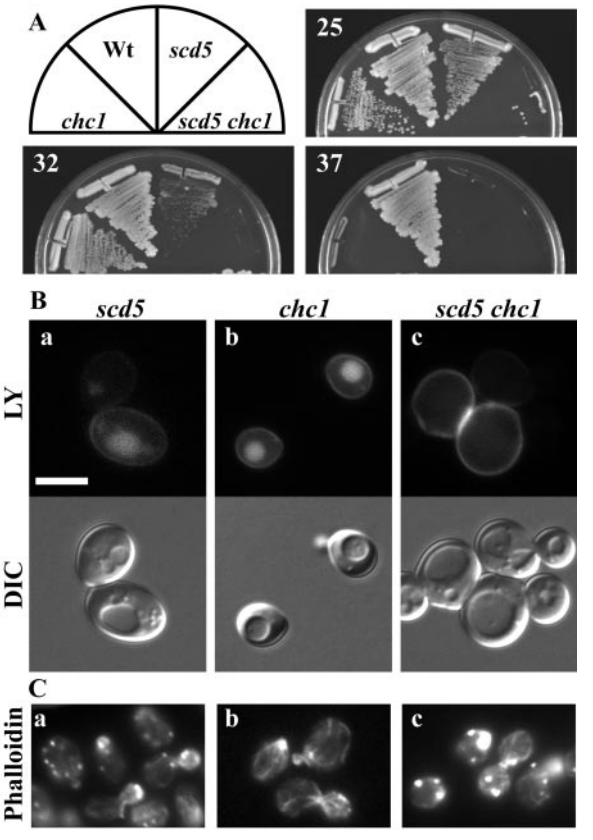

Figure 7. Synthetic phenotypes are caused by combining *scd5-Δ338* and *chc1-521*. (A) Growth of *scd5-Δ338 chc1-521* double mutant. SL4182 (*scd5-Δ338*) was crossed to SL2726 (*chc1-521*) and subjected to tetrad analysis. Resulting spore clones were streaked onto YEPD plates and incubated for 3 d at 25, 32, and 37°C. An example of a tetratype tetrad is shown. (B) Lucifer yellow uptake defect in *scd5-Δ338 chc1-521* mutant. Cells were grown to log phase in liquid YEPD at 25°C and incubated for 60 min with LY at 25°C. Top panels: LY fluorescence; bottom panels: location of vacuoles revealed by DIC imaging. Strains are as follows: (a) *scd5-Δ338*, SL3740; (b) *chc1-521*, SL2726; and (c) *scd5-Δ338 chc1-521*, SL4304. Bar, 5 μm. (C) Actin phenotype is exacerbated by combining *scd5-Δ338* with *chc1-521*. Cells were grown to log phase at 25°C in liquid YEPD, stained with Alexa-568-phalloidin, and photographed as described in MATERIALS AND METHODS. Strains are the same as shown in B.

Clathrin and Scd5p Interact with Sla2p by Two-hybrid Analysis

A yeast two-hybrid screen was carried out to identify clathrin LC interacting proteins (see MATERIALS AND METHODS). Thirteen positive clones were obtained. Two of the clones contained C-terminal fragments of Chc1p including the LC binding domain (Liu *et al.*, 1995), as would be expected. The other 11 clones (representing five distinct isolates) contained various fragments of Sla2p coding sequences. Figure 8A shows two-hybrid interaction results with two of the LC interacting Sla2p clones. The smallest Sla2p prey coded for amino acids 292–520, which includes part of the predicted central coil-coiled domain as well as the glutamine-rich region, the leucine zipper, and a portion of the proline-rich region (Figure 8B; Wesp *et al.*, 1997; Yang *et al.*, 1999). A slightly smaller fragment (residues 292–501) also interacted with LC (Figure 8A). Interestingly, similar regions in the related mammalian proteins, HIP1 and HIP1R, were recently shown to interact with clathrin (Engqvist-Goldstein *et al.*, 2001; Metzler *et al.*, 2001; Mishra *et al.*, 2001; Waelter *et al.*, 2001). Chc1p-655–1653, which binds LC, also interacted with Sla2p-292–501. However, this association was somewhat weaker than the interaction of LC with HC or LC with the Sla2p coil domain, as the pGAD-*CHC1-655*–1653/pGBD-*SLA2-292*–501 transformant grew consistently more slowly on the C-adenine reporter plates. This suggests that the interaction of HC with Sla2p might be through LC. In addition, confirming previous studies (Wesp *et al.*, 1997; Yang *et al.*, 1999), we found that the coil-coiled domain of Sla2p can interact with itself (Figure 8A).

Genetic interactions were also observed between clathrin mutations and *sla2*, supporting the two-hybrid physical as-

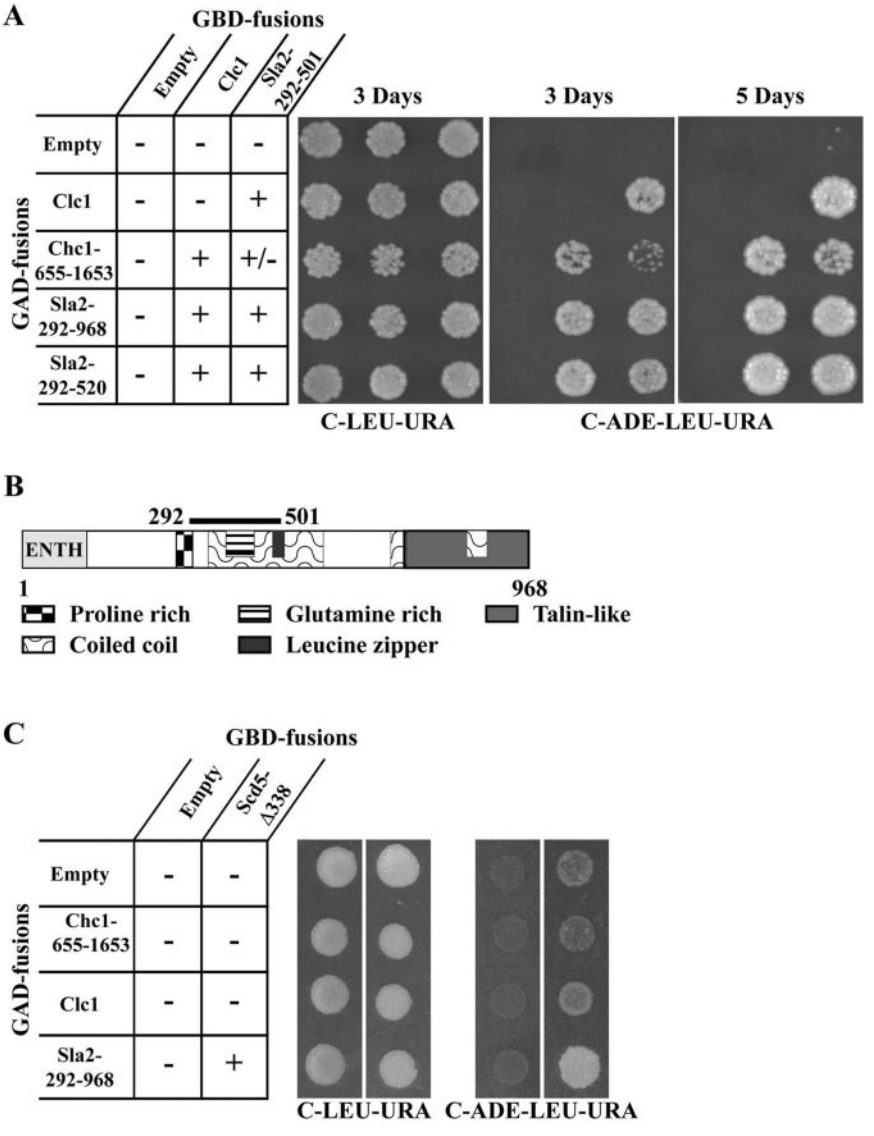

Figure 8. Clathrin and Scd5p interact with Sla2p by two-hybrid analysis. (A) Yeast strain YPJ96-4 was transformed with GAL4 binding domain (GBD) bait plasmids pGBDU (empty), pKH19 (GBD-*CLC1*), or pKH47 (GBD-*SLA2-292–501*) in combination with GAL4 activation domain (GAD) prey plasmids pGAD (empty), pKH24 (GAD-*CHC1-655–1653*), pKH19 (GAD-*CLC1*), p31-10 (GAD-*SLA2-292–968*), or p31-2 (GAD-*SLA2-292–520*). Equal numbers of cells from transformants were spotted on complete synthetic medium lacking leucine and uracil (C-LEU-URA) and medium lacking adenine, leucine, and uracil (C-ADE-LEU-URA) and grown for 3 and 5 d. Interactions of baits and preys were scored for activation of the *GAL2:: ADE2* reporter by growth on C-ADE-LEU-URA. (B) Model of Sla2p. Sla2p domains and region that associates with clathrin are indicated. (C) YPJ96-4 was transformed with GAL4 binding domain bait plasmids pGBDU (empty) or pNT1 (GBD-*scd5-Δ338*). SL3004 was transformed with GAL activation domain (GAD) plasmids pGAD (empty), pKH24 (GAD-*CHC1-655–1653*), pKH19 (GAD-*CLC1*), p31-10 (GAD-*SLA2-292–968*). Bait and prey plasmids were combined by the mating method. Cells were spotted on plates as described in A and grown for 3 d.

sociation results. Crosses of *chc1* mutants to *sla2* mutants resulted in strong synergistic growth phenotypes in double mutant spore progeny (Figure 9). In fact, *chc1*Δ was synthetically lethal with *sla2*Δ (Figure 9A). Similar results were observed when *clc1*Δ was combined with *sla2* mutations. Overall these results suggest that clathrin and Sla2p function in related pathways.

Because *scd5-Δ338* shows synthetic lethality with *sla2-41 (end4-1)* (Table 3) and strong genetic interactions with *chc1-521* (Figure 7), we tested whether Scd5p interacts with clathrin or Sla2p by two-hybrid analysis. When full-length Scd5p was fused with the GAL4 DNA binding domain (GBD), the fusion protein activated reporter genes even in the absence of the GAL4 activation domain (GAD) preys. However, the GBD-Scd5-Δ338 truncation only weakly autoactivated, allowing tests for interaction with Sla2p and clathrin preys. We found that Scd5-Δ338p could not interact with full-length LC or Chc1p-655–1653 (Figure 8C). However, a two-hybrid interaction was observed with the longer Sla2p-292–968 clone (Figure 8C) but not the Sla2p 292–520 fragment. Thus, the N-terminal region of Scd5p appears to associate with Sla2p, but this interaction depends on sequences C-terminal to the minimal region that binds clathrin LC.

Clathrin and Scd5p Are Required for Normal Sla2p Localization

In wild-type cells, Sla2p partially colocalizes with cortical actin patches (Yang *et al.*, 1999). This is most easily observed in unbudded and small budded cells where actin is highly polarized. Interestingly, not all actin patches stain with anti-Sla2p nor does every Sla2p patch have associated actin (Yang *et al.*, 1999; Figure 10, A and B). Because Scd5p and Chc1p interact with Sla2p by two-hybrid analysis, we tested whether Sla2p localization is affected in *scd5-Δ338* or

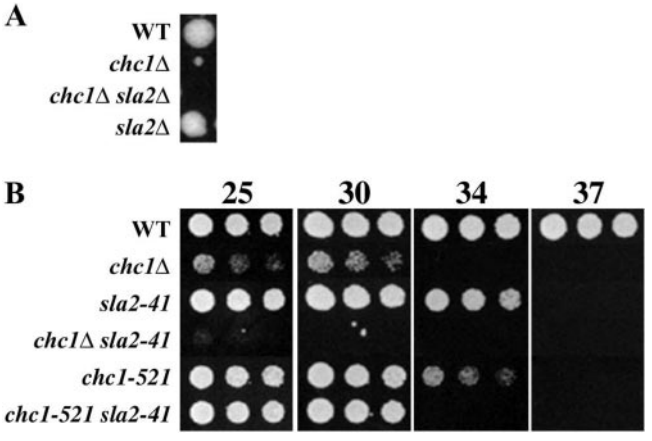

Figure 9. Clathrin mutants display negative synergistic growth defects with *sla2*. (A) *sla2*Δ and *chc1*Δ are synthetically lethal. SL4162 (*sla2*Δ) was crossed to SL13 (*chc1*Δ *scd1-v* YCp50-*CHC1*). The *CHC1* plasmid was dropped, and the diploid was sporulated and dissected for tetrad analysis. An example of a tetratype tetrad is shown. (B) Tetrads were dissected from SL13 (*chc1*Δ *scd1-v* YCp50-*CHC1*) X SL4049 (*sla2-41*) that had lost YCp50-*CHC1* or SL2726 (*chc1-521*) X SL4049. Overnight cultures of spore segregants were diluted to 10^7 cells/ml, and serial fourfold dilutions were made in YEPD. Equal volumes of cells were spotted on YEPD and plates were grown for 2 d at the indicated temperatures.

Chc1p-depleted cells. In *scd5*-Δ*338* cells grown at 25°C, Sla2p was partially delocalized to the cytoplasm, but there was still some residual cortical staining of Sla2p (Figure 10, C and D). This remaining cortical Sla2p was much less polarized than in wild-type cells, and less was found in actin patches (Figure 10, C, D, and M). After a 3-h shift to 34°C, nearly all of the Sla2p was cytoplasmic, although faint cortical rim staining was observed in some *scd5*-Δ*338* cells (Figure 10F). However, these small patches at the cell periphery rarely colocalized with actin (Figure 10M). When *GAL1::CHC1* cells were depleted of clathrin by growth on glucose, Sla2p was completely cytoplasmic in most cells (Figure 10, H and M), whereas cells grown on galactose showed the normal Sla2p staining pattern.

We also localized another cortical actin patch protein, Abp1p (Drubin *et al.*, 1988), which was tagged with GFP. Interestingly, in the majority of *scd5*-Δ*338* cells grown at either 25 or 34°C, as well as cells depleted of clathrin, GFP-Abp1p was still associated with actin patches (Figure 10, I–M). Similar results were obtained with Rvs167p. Thus, loss of Scd5p or clathrin function specifically affects Sla2p and does not cause a general effect on all cortical patch proteins.

DISCUSSION

Scd5p Plays a Role in Actin Organization and Endocytosis

In this study we found that Scd5p is crucial for normal actin organization and endocytosis. Both fluid-phase and receptor-mediated endocytosis were completely blocked in the *scd5*-Δ*338* mutant at the nonpermissive temperature, which is a phenotype caused by many mutations that affect the cortical actin cytoskeleton. In these cells cortical actin patches were often larger or depolarized to the mother cell, and a major accumulation of G-actin in bar structures was observed, suggesting a defect in actin assembly or destabilization of F-actin. Other phenotypes typical of mutants with actin defects were observed in *scd5*-Δ*338* (Pruyne and Bretscher, 2000a, 2000b), including delocalized chitin deposition, bud site selection defects, thickened cell walls, and the presence of multibudded and multinucleated cells. Supporting the phenotypic analysis, Scd5p colocalized with actin patches in the cell.

In our previous work on *SCD5* we showed that the *scd5*-Δ*338* mutation caused a partial post-Golgi secretory defect at the nonpermissive temperature (Nelson *et al.*, 1996). Based on the evidence presented here, this secretory defect could be due to the effect of loss of Scd5p function on the actin cytoskeleton and/or endocytosis. Several other actin patch mutants display similar partial secretory defects or accumulation of secretory vesicles, including *act1-1*, *myo3*Δ *myo5*Δ, *sla2*Δ, *rvs161*Δ, and *rvs167*Δ (Novick and Botstein, 1985; Goodson *et al.*, 1996; Mulholland *et al.*, 1997; Breton *et al.*, 2001). Budding continues and secretory vesicles still polarize to growth sites in many of these patch mutants, including *scd5*-Δ*338* (K. Henry, unpublished results). It has been suggested that a defect in endocytosis may affect recycling of components (e.g., v-SNAREs) required for assembly of mature fusion-competent secretory vesicles (Pruyne and Bretscher, 2000a). However, we noted that the *scd5* mutant had cables that were often misoriented within the cell, so the secretion phenotypes could be due to a partial effect on polarization of actin cables. This polarization defect might be caused indirectly by effects on cortical actin patches, which may contribute to anchoring of cables in the bud. Alternatively endocytic defects might affect localization of important membrane proteins that provide cues needed for cable polarization. A more complex function for Scd5p is suggested by the *scd5*-Δ*338* budding pattern defect. Unlike most cortical patch mutants, which show defects only in the diploid bipolar budding pattern (Yang *et al.*, 1997; Pruyne and Bretscher, 2000a), *scd5*-Δ*338* was defective in both haploid and diploid specific budding. Also *SCD5* is an essential gene, whereas many cortical actin patch components that affect endocytosis are not. This suggests that Scd5p could play a broader role in actin organization and cell polarization or may function in other cellular processes unrelated to actin.

scd5-Δ338 *Shows Genetic Interactions with Mutations in Genes Encoding Other Cortical Actin Patch Components*

We found that the *scd5*-Δ*338* mutation caused more severe growth and actin organization phenotypes when combined with a number of mutations in cortical actin patch components, supporting the idea that Scd5p is important for cortical actin function. Interestingly, *scd5*-Δ*338* was synthetically lethal with *pan1-20* and *end3*Δ but phenotypes were not exacerbated with *sla1*Δ, even although Pan1p, End3p, and Sla1p exist in a complex (Tang *et al.*, 2000; Zeng *et al.*, 2001). This difference could be explained by the fact that *pan1* and *end3*Δ mutants have severe endocytic phenotypes (Bénédetti *et al.*, 1994; Tang *et al.*, 1997; Duncan *et al.*, 2001), whereas

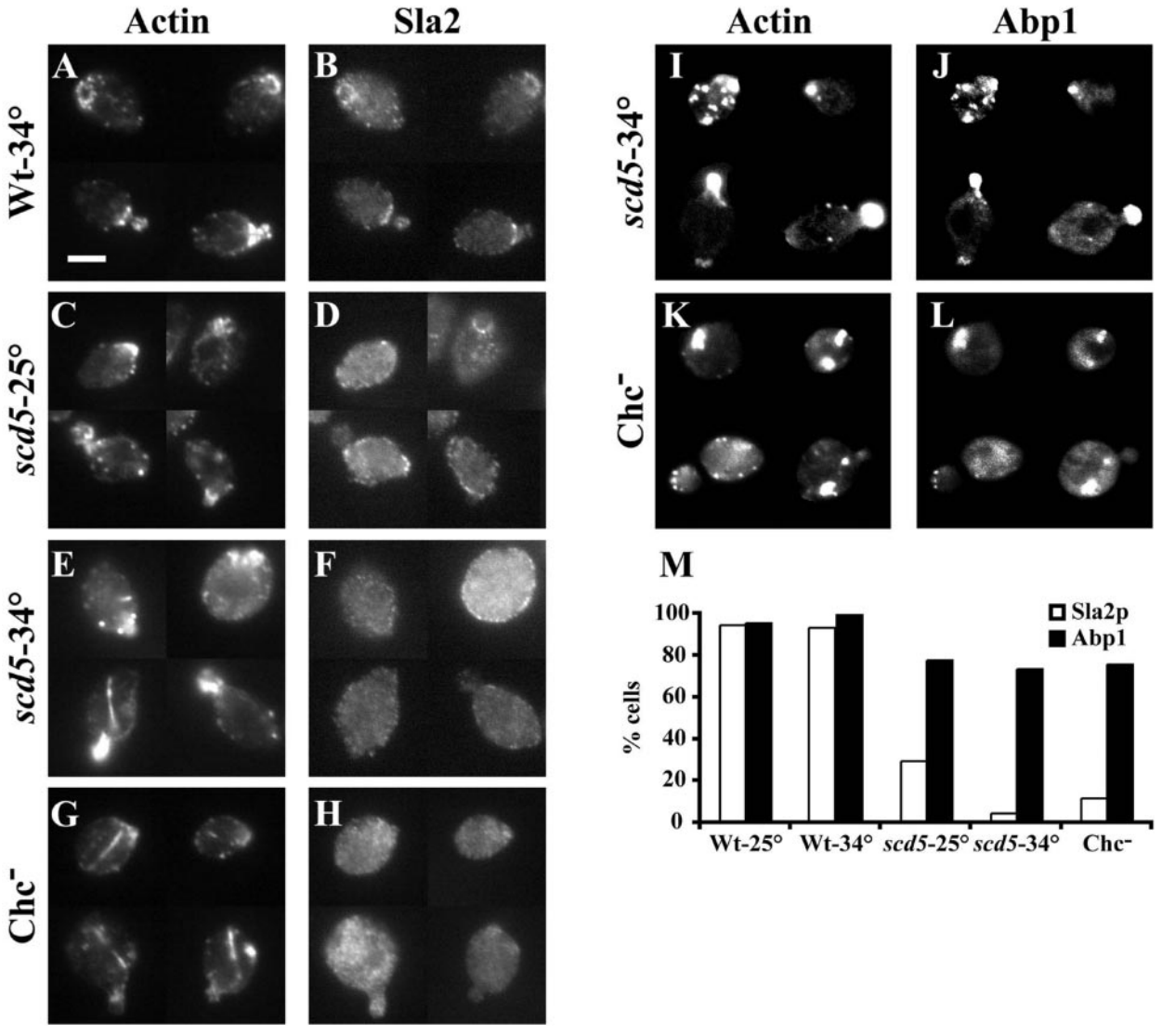

Figure 10. Sla2p is mislocalized in *scd5*-Δ*338* and clathrin-depleted cells. Wild-type (SL1528; A and B) and *scd5*-Δ*338* (SL3920; C–F) strains were grown on YEPD to log phase at 25°C (C and D) or shifted to 34°C (A, B, E, F) for 3 h. The *GAL1:: CHC1* strain (SL554; G and H) was grown to log phase in YEP-GAL and then shifted to YEPD for 15 h at 30°C to deplete clathrin HC. In I and J *scd5*-Δ*338* (SL3920) + pJC4 [pGFP-ABP1] was grown in C-URA and shifted to 34°C for 3 h. In K and L the *GAL1: CHC1* strain (SL554) + pJC4 [pGFP-ABP1] was grown in C-URA+GAL and then shifted to glucose medium for 15 h to deplete clathrin HC. Cells were fixed, stained with anti-actin (A, C, E, and G) and anti-Sla2p antibodies (B, D, F, and H); or in cells for GFP-Abp1p localization (J and L) actin was visualized with Alexa-594 phalloidin (I and K). (M) Quantification of the percent of cells with Sla2p or Abp1p showing colocalization with actin patches. Note that the *GAL1*::*CHC1* strain grown on galactose gave similar results as wild-type cells. Bar, 5 μm.

*sla1*Δ is only modestly affected (Ayscough *et al.*, 1999; K. Henry, unpublished results). Because interaction of End3p with Pan1p is not dependent on the presence of Sla1p (Tang *et al.*, 2000), perhaps Pan1p and End3p association are most critical for function of this complex. Also, *END3*, but not *SLA1*, overexpression rescues the temperature sensitivity of *pan1-4*, and overexpression of *SLA1* prevents *END3* overexpression from rescuing the *pan1* mutant at 37°C (Tang *et al.*, 2000). Thus, Sla1p may act antagonistically to End3p, which could explain the difference in genetic interactions with *scd5*-Δ*338*.

scd5-Δ*338* had a strong genetic interaction with *abp1*Δ and *rvs167*Δ, but not *srv2*Δ. Interestingly both Srv2p (adenylyl cyclase–associated protein) and Rvs167p interact with Abp1p (Freeman *et al.*, 1996; Lila and Drubin, 1997; Drees *et al.*, 2001; Fazi *et al.*, 2001). However, *rvs167*Δ, but not *srv2*Δ, shows a pattern of genetic interactions similar to *abp1*Δ when combined with other mutations in genes encoding actin cytoskeleton components (Lila and Drubin, 1997). Thus, the results with *scd5*-Δ*338* further support the idea that Abp1p and Rvs167p functions are closely related.

Sla2p Localization Is Dependent on Scd5p

Scd5p is also physically associated with components of the cortical actin cytoskeleton. In addition to showing overlapping localization with cortical actin patches, Scd5p interacts with Sla2p by two-hybrid analysis. In preliminary studies, we find that it also interacts with Rvs167p, but not Rvs161p, by two-hybrid screening (J. Chang, unpublished results). Thus far we have not been able to demonstrate association of Sla2p and Scd5p by coprecipitation, but their interaction may be transient or only occur in the context of the plasma membrane or when assembled with cortical actin structures. However, based on the synthetic lethality caused by combining *sla2-41* (*end4-1*) with *scd5-Δ338*, we believe the physical interactions detected by two-hybrid analysis are functionally important. As further support for this, we found that Sla2p dissociated from cortical structures and accumulated in the cytoplasm in *scd5-Δ338* cells. The delocalization of Sla2p seen in *scd5-Δ338* appears to be specific, because other actin patch-associated components, Abp1p and Rvs167p, localize in cortical sites relatively normally in these cells. Also, *scd5-Δ338* cells still have phalloidin-staining actin patch-like structures, indicating the effect of *scd5-Δ338* on Sla2p localization is not merely caused by actin depolymerization.

It is interesting to note that although Scd5-Δ338p associates with Sla2p by two-hybrid interaction, the same truncation mutation causes delocalization of Sla2p. Possibly the C-terminal region of Scd5p is important for its localization with cortical actin, and perturbation of Scd5p localization thereby affects Sla2p's association with actin patches.

Scd5p has also been shown to interact with Glc7p (Tu *et al.*, 1996; Uetz *et al.*, 2000; Venturi *et al.*, 2000; JiSuk Chang, unpublished results), which is yeast PP1, a broad specificity Ser/Thr phosphatase with many cellular functions (Stark, 1996). PP1's activity is restricted toward physiological substrates in vivo by different regulatory or targeting subunits (Stark, 1996), so it is possible that Scd5p targets PP1 to dephosphorylate specific actin-associated components. It could play a major role in regulating assembly, disassembly, or specific organization of actin-associated factors needed for endocytosis. Supporting this idea, genetic interactions with *scd5-Δ338* were observed with mutations in a number of actin-associated proteins that are known to be phosphorylated. One of these proteins is Sla2p, which interacts with Ark1p, an actin regulating kinase (ARK; Cope *et al.*, 1999). Pan1p and Sla1p are phosphorylated by Prk1p (another ARK), as well as Ark1p (Zeng and Cai, 1999; Zeng *et al.*, 2001). Recent evidence indicates that Prk1p phosphorylation disrupts association of Pan1p with Sla1p and End3p (Zeng *et al.*, 2001). Also, in *ark1Δ prk1Δ* double mutants cortical F-actin patches, and many patch components, including Sla2p, are found in large aggregates (Cope *et al.*, 1999). Because we find that Sla2p dissociates from the cortex in the *scd5-Δ338* mutant, dephosphorylation of Sla2p or other patch components may be important for assembly in actin patches, and Scd5p/PP1 may regulate this.

Clathrin Is Important for Organization of Actin in Yeast

In previous studies we identified *SCD5* as a multicopy suppressor of clathrin-deficient yeast, but *scd5-Δ338* cells do not show the Golgi retention defects that lead to CPY sorting and alpha factor processing phenotypes seen in clathrin mutants (Nelson *et al.*, 1996). Also, overexpression of *SCD5* could not suppress these clathrin mutant phenotypes (Nelson and Lemmon, 1993). Here we report our discovery that clathrin mutants, like *scd5-Δ338* cells, have major cortical actin defects and accumulate significant nonfilamentous G-actin. *SCD5* overexpression partially suppressed these actin defects, and combining *scd5-Δ338* with a *chc1-ts* mutation exacerbated growth, actin and endocytic phenotypes. Furthermore, clathrin mutations genetically interact with *sla2* mutations, and Sla2p association with the cortex is dependent on the presence of clathrin. Previous studies are also consistent with a connection between clathrin and actin in yeast. Clathrin-deficient yeast become polyploid at high frequency, and aberrant nuclear divisions within the mother cell are observed (Lemmon and Jones, 1987; Lemmon *et al.*, 1990). Like *scd5-Δ338* and other actin patch mutants, clathrin mutants are enlarged and round in appearance, they have delocalized chitin deposition, and their cell walls are thickened (Lemmon and Jones, 1987; Lemmon *et al.*, 1990; S.K. Lemmon, unpublished results). Moreover, clathrin interacts with other cortical patch components, such as Ent1/2p (Wendland *et al.*, 1999), in addition to Sla2p. Therefore, we suggest that clathrin plays a role in cortical actin function in yeast.

Clathrin Interacts with Sla2p

Clathrin is a trimeric molecule with three HC's joined at the C terminus and a LC bound to each leg in the hub region adjacent to the triskelion vertex. Each HC contains an N-terminal globular terminal domain (TD) that interacts with a number of proteins containing a signature clathrin binding motif ("clathrin box") related to LLDLD in amphiphysin (Dell'Angelica, 2001). This interaction is thought to facilitate the recruitment of clathrin and many of its associated factors to sites of clathrin-mediated transport. The yeast epsins (Ent1/2p) and AP180-like proteins (Yap1801p/Yap1802p) both bind to the Chc1p TD via this type of clathrin binding motif (Wendland and Emr, 1998; Wendland *et al.*, 1999). Interestingly, we identified Sla2p in a two-hybrid screen with the clathrin LC. Although Sla2p has some sequences distantly related to the LLDLD motif, we found that the clathrin LC interacted with a portion of the Sla2p central coiled-coil domain, which does not contain potential clathrin TD-binding sequences. A fragment of clathrin HC including the LC binding region, but not the TD, also interacted with Sla2p, albeit more weakly than LC. In preliminary studies we find that LC interacts with Sla2p by two-hybrid analysis in a *chc1Δ* strain, indicating that this association is not dependent on HC (T. Newpher, unpublished results). We note that, because Sla2p dimerizes via the central coiled-coil domain (Wesp *et al.*, 1997; Yang *et al.*, 1999; this study), the two-hybrid coiled-coil product could associate with endogenous Sla2p. Thus, we cannot yet exclude the possibility that the LC interacts with another portion of Sla2p or that clathrin HC interacts with other Sla2p regions, possibly via the TD. However, consistent with an importance for the LC-Sla2p coiled-coil interaction, deletion of the Sla2p central coiled-coil domain causes defects in endocytosis and actin organization that resemble those of clathrin-deficient cells (Wesp *et al.*, 1997; Yang *et al.*, 1999).

Recent work has shown that the mammalian Sla2p-related proteins, HIP1 and HIP1R, localize to sites of clathrin-mediated endocytosis in vivo, are enriched in clathrin-coated vesicles, and bind directly to clathrin (Engqvist-Goldstein *et al.*, 1999, 2001; Metzler *et al.*, 2001; Mishra *et al.*, 2001; Waelter *et al.*, 2001). Additional studies indicate that that HIP1R may link the actin cytoskeleton to coated pits and suggest that cortical actin helps organize or isolate regions of active clathrin-mediated internalization (Gaidarov *et al.*, 1999; Bennett *et al.*, 2001; Engqvist-Goldstein *et al.*, 2001). Thus, HIP1(R) may be important for this organization of coated-pits or may be actively involved in the endocytic process itself.

The binding of clathrin to HIP1 and HIP1R appear to be distinct. In HIP1, there are clathrin N-TD-binding sequences as well as AP-2 binding motifs (DPF and FXDXF) adjacent to the central coiled-coil region (Metzler *et al.*, 2001; Mishra *et al.*, 2001; Waelter *et al.*, 2001). In HIP1R the binding to clathrin appears to occur principally via the coil-coiled region and involves a direct interaction with clathrin LC (Engqvist-Goldstein *et al.*, 2001; Legendre-Guillemin *et al.*, 2002), similar to our findings of Sla2p and yeast LC binding. In addition, overexpression of a hub fragment of clathrin, which contains the LC binding site and inhibits clathrin-mediated endocytosis, causes dissociation of HIP1R from coated pits in HeLa cells (Bennett *et al.*, 2001). Similarly, we found that depletion of clathrin causes dissociation of Sla2p from the cell cortex. Overall this indicates there are close connections between clathrin, Sla2p-related proteins and the actin cytoskeleton in all eukaryotes.

Why then might clathrin deficiency in yeast only cause a partial defect in endocytosis? Clathrin may help collect specific membrane proteins, localize regulatory factors and or mark/domains for endocytosis, but not be absolutely required for generating force for internalization, which may be primarily an actin-mediated process in yeast. Clathrin may be diffusely distributed in the cortical actin network, which would explain why surface-coated pits have yet to be detected by microscopic methods. Possibly, classic surface-derived CCV do not even form in yeast, although some plasma membrane proteins have been detected in enriched CCV fractions (Pishvaee *et al.*, 2000). Still, it has not been ruled out that these vesicles are of endosomal origin or on a recycling trajectory (Valdivia *et al.*, 2002). Recent work also indicates that clathrin may be important for formation of a subclass of secretory vesicles, so CCV could contain newly synthesized plasma membrane proteins (Gurunathan *et al.*, 2002; Harsay and Schekman, 2002). Nonetheless, our findings suggest that the endocytic phenotype of clathrin-deficient cells may relate to a role for clathrin in actin-associated processes. This effect may only be partial because clathrin is one of several factors that facilitate organization or stabilization of the cortical actin network. Interestingly, many homologues of mammalian clathrin associated factors that are involved in endocytosis in yeast (e.g., Ent1/2p [epsins], Pan1p [Eps15-related], and Rvs161 and Rvs167 [amphiphysins]), are also important for actin organization (Munn *et al.*, 1995; Sivadon *et al.*, 1995; Tang and Cai, 1996; Wendland *et al.*, 1996; Balguerie *et al.*, 1999; Wendland *et al.*, 1999).

A final question concerns why *SCD5* was isolated as a multicopy suppressor of clathrin-deficient lethality. Mutations in both clathrin and *SCD5* show genetic interactions with *sla2* and both clathrin and Scd5p are required for localization of Sla2p at the cell cortex. Our data suggest that Scd5p, as a potential targeting subunit for PP1, may promote the recruitment of proteins, like Sla2p, to the cortical actin network. Thus, overexpression of *SCD5* could counter the destabilization of cortical actin components that might occur in the absence of clathrin. Further studies will be directed toward determining whether Scd5p plays a regulatory role in actin organization and endocytosis and determining what are its targets.

ACKNOWLEDGMENTS

We thank David Drubin, Mark Rose, Beverly Wendland, Clarence Chan, and Scott Vande Pol for kindly providing strains, plasmids, and antibodies. The authors also thank Dan Gelperin, Jo Ann Wise, and Susann Brady-Kalnay for their advice and many helpful discussions and Maryanne Pendergast for help with confocal microscopy. K.R.H. was supported by a National Institutes of Health (NIH) training grant (T32 AG00105) and an individual National Research Service Award (NRSA) Minority Predoctoral Fellowship (F31 GM20082). K.H. was the recipient of an NRSA postdoctoral fellowship (F32 GM17370) from NIH. R.T.H. was supported by NIH training grant (T32 DK7319-23). This work was funded by the NIH (R01 GM55796) and the American Cancer Society (RPG-9403104-MBC to S.K.L.), the Canton Basel-Stadt and the Swiss National Science Foundation (H.R.), and the Roche Research Foundation (S.K.L. and H.R.). S.K.L. was the recipient of a Career Advancement Award from the National Science Foundation.

REFERENCES

Adams, A.E., Botstein, D., and Drubin, D.G. (1991). Requirement of yeast fimbrin for actin organization and morphogenesis in vivo. Nature *354*, 404–408.

Adams, A.E., and Pringle, J.R. (1984). Relationship of actin and tubulin distribution to bud growth in wild- type and morphogenetic-mutant *Saccharomyces cerevisiae*. J. Cell Biol. *98*, 934–945.

Adams, A.E., and Pringle, J.R. (1991). Staining of actin with fluorochrome-conjugated phalloidin. Methods Enzymol. *194*, 729–731.

Apodaca, G. (2001). Endocytic traffic in polarized epithelial cells: role of the actin and microtubule cytoskeleton. Traffic *2*, 149–159.

Ayscough, K.R., Eby, J.J., Lila, T., Dewar, H., Kozminski, K.G., and Drubin, D.G. (1999). Sla1p is a functionally modular component of the yeast cortical actin cytoskeleton required for correct localization of both Rho1p-GTPase and Sla2p, a protein with talin homology. Mol. Biol. Cell *10*, 1061–1075.

Ayscough, K.R., Stryker, J., Pokala, N., Sanders, M., Crews, P., and Drubin, D.G. (1997). High rates of actin filament turnover in budding yeast and roles for actin in establishment and maintenance of cell polarity revealed using the actin inhibitor latrunculin-A. J. Cell Biol. *137*, 399–416.

Baggett, J.J., and Wendland, B. (2001). Clathrin function in yeast endocytosis. Traffic *2*, 297–302.

Balguerie, A., Sivadon, P., Bonneu, M., and Aigle, M. (1999). Rvs167p, the budding yeast homolog of amphiphysin, colocalizes with actin patches. J. Cell Sci. *112*, 2529–2537.

Bauer, F., Urdaci, M., Aigle, M., and Crouzet, M. (1993). Alteration of a yeast SH3 protein leads to conditional viability with defects in cytoskeletal and budding patterns. Mol. Cell. Biol. *13*, 5070–5084.

Bénédetti, H., Raths, S., Crausaz, F., and Riezman, H. (1994). The *END3* gene encodes a protein that is required for the internalization

step of endocytosis and for actin cytoskeleton organization in yeast. Mol. Biol. Cell *5*, 1023–1037.

Benmerah, A., Begue, B., Dautryvarsat, A., and Cerfbensussan, N. (1996). The ear of alpha-adaptin interacts with the COOH-terminal domain of the Eps15 protein. J. Biol. Chem. *271*, 12111–12116.

Bennett, E.M., Chen, C.-Y., Engqvist-Goldstein, A.E.Y., Drubin, D.G., and Brodsky, F.M. (2001). Clathrin hub expression dissociates the actin binding protein Hip1R from coated pits and disrupts their alignment with the actin cytoskeleton. Traffic *2*, 851–858.

Botstein, D., Amberg, D., Mullholland, J., Huffaker, T., Adams, A., Drubin, D., and Stearns, T. (1997). The yeast cytoskeleton. In: The Molecular and Cellular Biology of the Yeast *Saccharomyces*: Cell Cycle and Cell Biology, vol. 3, ed. J.R. Pringle, J.R. Broach, and E.W. Jones, Cold Spring Harbor, NY: Cold Spring Harbor Laboratory Press, 1–90.

Botstein, D., Falco, S.C., Stewart, S.E., Brennan, M., Scherer, S., Stinchcomb, D.T., Struhl, K., and Davis, R.W. (1979). Sterile host yeasts (SHY): a eukaryotic system of biological containment for recombinant DNA experiments. Gene *8*, 17–24.

Breton, A.M., Schaeffer, J., and Aigle, M. (2001). The yeast Rvs161 and Rvs167 proteins are involved in secretory vesicles targeting the plasma membrane and in cell integrity. Yeast *18*, 1053–1068.

Brodsky, F.M., Chen, C.Y., Knuehl, C., Towler, M.C., and Wakeham, D.E. (2001). Biological basket weaving. Formation and function of clathrin-coated vesicles. Annu. Rev. Cell Dev. Biol. *17*, 517–568.

Chen, H., Fre, S., Slepnev, V.I., Capua, M.R., Takei, K., Butler, M.H., Di Fiore, P.P., and De Camilli, P. (1998). Epsin is an EH-domain-binding protein implicated in clathrin-mediated endocytosis. Nature *394*, 793–797.

Cope, M.J., Yang, S., Shang, C., and Drubin, D.G. (1999). Novel protein kinases Ark1p and Prk1p associate with and regulate the cortical actin cytoskeleton in budding yeast. J. Cell Biol. *144*, 1203–1218.

Cotton, R.G. (1992). Detection of mutations in DNA. Curr. Opin. Biotechnol. *3*, 24–30.

D'Hondt, K., Heese-Peck, A., and Riezman, H. (2000). Protein and lipid requirements for endocytosis. Annu. Rev. Genet. *34*, 255–295.

David, C., McPherson, P.S., Mundigl, O., and DeCamilli, P. (1996). A role of amphiphysin in synaptic vesicle endocytosis suggested by its binding to dynamin in nerve terminals. Proc. Natl. Acad. Sci. USA *93*, 331–335.

Dell'Angelica, E.C. (2001). Clathrin-binding proteins: got a motif? Join the network! Trends Cell Biol. *11*, 315–318.

DiFiore, P.P., Pelicci, P.G., and Sorkin, A. (1997). EH: a novel protein-protein interaction domain potentially involved in intracellular sorting. Trends Biochem. Sci. *22*, 411–413.

Drake, M.T., Downs, M.A., and Traub, L.M. (2000). Epsin binds to clathrin by associating directly with the clathrin-terminal domain. Evidence for cooperative binding through two discrete sites. J. Biol. Chem. *275*, 6479–6489.

Drees, B.L., *et al.* (2001). A protein interaction map for cell polarity development. J. Cell Biol. *154*, 549–576.

Drubin, D.G., Miller, K.G., and Botstein, D. (1988). Yeast actin-binding proteins: evidence for a role in morphogenesis. J. Cell Biol. *107*, 2551–2561.

Drubin, D.G., Mulholland, J., Zhu, Z.M., and Botstein, D. (1990). Homology of a yeast actin-binding protein to signal transduction proteins and myosin-I. Nature *343*, 288–290.

Dulic, V., Egerton, M., Elguindi, I., Raths, S., Singer, B., and Riezman, H. (1991). Yeast endocytosis assays. Methods Enzymol. *194*, 697–710.

Duncan, M.C., Cope, M.J., Goode, B.L., Wendland, B., and Drubin, D.G. (2001). Yeast Eps15-like endocytic protein, Pan1p, activates the Arp2/3 complex. Nat. Cell Biol. *3*, 687–690.

Engqvist-Goldstein, A.E., Kessels, M.M., Chopra, V.S., Hayden, M.R., and Drubin, D.G. (1999). An actin-binding protein of the Sla2/Huntingtin interacting protein 1 family is a novel component of clathrin-coated pits and vesicles. J. Cell Biol. *147*, 1503–1518.

Engqvist-Goldstein, A.E., Warren, R.A., Kessels, M.M., Keen, J.H., Heuser, J., and Drubin, D.G. (2001). The actin-binding protein Hip1R associates with clathrin during early stages of endocytosis and promotes clathrin assembly in vitro. J. Cell Biol. *154*, 1209–1224.

Fazi, B., *et al.* (2001). Unusual binding properties of the SH3 domain of the yeast actin binding protein Abp1: structural and functional analysis. J. Biol. Chem. *19*, 5290–5298.

Ford, M.G., Pearse, B.M., Higgins, M.K., Vallis, Y., Owen, D.J., Gibson, A., Hopkins, C.R., Evans, P.R., and McMahon, H.T. (2001). Simultaneous binding of PtdIns(4,5)P2 and clathrin by AP180 in the nucleation of clathrin lattices on membranes. Science *291*, 1051–1055.

Freeman, N.L., Lila, T., Mintzer, K.A., Chen, Z., Pahk, A.J., Ren, R., Drubin, D.G., and Field, J. (1996). A conserved proline-rich region of the *Saccharomyces cerevisiae* cyclase-associated protein binds SH3 domains and modulates cytoskeletal localization. Mol. Cell. Biol. *16*, 548–556.

Fujimoto, L.M., Roth, R., Heuser, J.E., and Schmid, S.L. (2000). Actin assembly plays a variable, but not obligatory role in receptor-mediated endocytosis in mammalian cells. Traffic *1*, 161–171.

Gagny, B., Wiederkehr, A., Dumoulin, P., Winsor, B., Riezman, H., and Haguenauer-Tsapis, R. (2000). A novel EH domain protein of *Saccharomyces cerevisiae*, Ede1p, involved in endocytosis. J. Cell Sci. *113*, 3309–3319.

Gaidarov, I., Santini, F., Warren, R.A., and Keen, J.H. (1999). Spatial control of coated-pit dynamics in living cells. Nat. Cell Biol. *1*, 1–7.

Gietz, R.D., Schiestl, R.H., Willems, A.R., and Woods, R.A. (1995). Studies on the transformation of intact yeast cells by the LiAc/SS-DNA/PEG procedure. Yeast *11*, 355–360.

Goodson, H.V., Anderson, B.L., Warrick, H.M., Pon, L.A., and Spudich, J.A. (1996). Synthetic lethality screen identifies a novel yeast myosin I gene (MYO5): myosin I proteins are required for polarization of the actin cytoskeleton. J. Cell Biol. *133*, 1277–1291.

Gurunathan, S., David, D., and Gerst, J.E. (2002). Dynamin and clathrin are required for the biogenesis of a distinct class of secretory vesicles in yeast. EMBO J. *21*, 602–614.

Guthrie, C., and Fink, G.R. (1991). Guide to Yeast Genetics and Molecular Biology. San Diego: Academic Press, 933 pp.

Harper, J.W., Adami, G.R., Wei, N., Keyomarsi, K., and Elledge, S.J. (1993). The p21 Cdk-interacting protein Cip1 is a potent inhibitor of G1 cyclin-dependent kinases. Cell *75*, 805–816.

Harsay, E., and Schekman, R. (2002). A subset of yeast vacuolar protein sorting mutants is blocked in one branch of the exocytic pathway. J. Cell Biol. *156*, 271–285.

Heil-Chapdelaine, R.A., Tran, N.K., and Cooper, J.A. (1998). The role of *Saccharomyces cerevisiae* coronin in the actin and microtubule cytoskeletons. Curr. Biol. *8*, 1281–1284.

Holtzman, D.A., Yang, S., and Drubin, D.G. (1993). Synthetic-lethal interactions identify two novel genes, *SLA1* and *SLA2*, that control membrane cytoskeleton assembly in *Saccharomyces cerevisiae*. J. Cell Biol. *122*, 635–644.

Huang, K.M., Gullberg, L., Nelson, K.K., Stefan, C.J., Blumer, K., and Lemmon, S.K. (1997). Novel functions of clathrin light chains: clathrin heavy chain trimerization is defective in light chain-deficient yeast. J. Cell Sci. *110*, 899–910.

Iannolo, G., Salcini, A.E., Gaidarov, I., Goodman, O.B., Baulida, J., Carpenter, G., Pelicci, P.G., DiFiore, P.P., and Keen, J.H. (1997). Mapping of the molecular determinants involved in the interaction between Eps15 and AP-2. Cancer Res. *57*, 240–245.

Itoh, T., Koshiba, S., Kigawa, T., Kikuchi, A., Yokoyama, S., and Takenawa, T. (2001). Role of the ENTH domain in phosphatidylinositol-4,5-bisphosphate binding and endocytosis. Science *291*, 1047–1051.

James, P., Halladay, J., and Craig, E.A. (1996). Genomic libraries and a host strain designed for highly efficient two-hybrid selection in yeast. Genetics *144*, 1425–1436.

Kalchman, M.A., *et al.* (1997). HIP1, a human homologue of *S. cerevisiae* Sla2p, interacts with membrane-associated huntingtin in the brain. Nat. Genet. *16*, 44–53.

Kessels, M.M., Engqvist-Goldstein, A.E., Drubin, D.G., and Qualmann, B. (2001). Mammalian Abp1, a signal-responsive F-actin-binding protein, links the actin cytoskeleton to endocytosis via the GTPase dynamin. J. Cell Biol. *153*, 351–366.

Kübler, E., and Riezman, H. (1993). Actin and fimbrin are required for the internalization step of endocytosis in yeast. EMBO J. *12*, 2855–2862.

Kunkel, T.A., Roberts, J.D., and Zakour, R.A. (1987). Rapid and efficient site-specific mutagenesis without phenotypic selection. Methods Enzymol. *154*, 367–382.

Legendre-Guillemin, V., Metzler, M., Charbonneau, M., Gan, L., Chopra, V., Philie, J., Hayden, M.R., and McPherson, P.S. (2002). HIP1 and HIP12 display differential binding to F-actin, AP2, and clathrin: identification of a novel interaction with clathrin-light chain. J. Biol. Chem. *277*, 19897–19904.

Lemmon, S.K., Freund, C., Conley, K., and Jones, E.W. (1990). Genetic instability of clathrin-deficient strains of *S. cerevisiae*. Genetics *124*, 27–38.

Lemmon, S.K., and Jones, E.W. (1987). Clathrin requirement for normal growth of yeast. Science *238*, 504–509.

Lila, T., and Drubin, D.G. (1997). Evidence for physical and functional interactions among two *S. cerevisiae* SH3 domain proteins, an adenylyl cyclase-associated protein and the actin cytoskeleton. Mol. Biol. Cell *8*, 367–385.

Liu, S.H., Wong, M.L., Craik, C.S., and Brodsky, F.M. (1995). Regulation of clathrin assembly and trimerization defined using recombinant triskelion hubs. Cell *83*, 257–267.

Madania, A., Dumoulin, P., Grava, S., Kitamoto, H., Scharer-Brodbeck, C., Soulard, A., Moreau, V., and Winsor, B. (1999). The *S. cerevisiae* homologue of human Wiskott-Aldrich syndrome protein Las17p interacts with the Arp2/3 complex. Mol. Biol. Cell *10*, 3521–3538.

McCann, R.O., and Craig, S.W. (1997). The I/LWEQ module: a conserved sequence that signifies F-actin binding in functionally diverse proteins from yeast to mammals. Proc. Natl. Acad. Sci. USA *94*, 5679–5684.

McClary, J.A., Witney, F., and Geisselsoder, J. (1989). Efficient site-directed in vitro mutagenesis using phagemid vectors. Biotechniques *7*, 282–289.

McMahon, H.T. (1999). Endocytosis: an assembly protein for clathrin cages. Curr. Biol. *9*, R332–R335.

McPherson, P.S., *et al.* (1996). A presynaptic inositol-5-phosphatase. Nature *379*, 353–357.

Metzler, M., Legendre-Guillemin, V., Gan, L., Chopra, V., Kwok, A., McPherson, P.S., and Hayden, M.R. (2001). HIP1 functions in clathrin-mediated endocytosis through binding to clathrin and adaptor protein 2. J. Biol. Chem. *276*, 39271–39276.

Mishra, S.K., Agostinelli, N.R., Brett, T.J., Mizukami, I., Ross, T.S., and Traub, L.M. (2001). Clathrin- and AP-2-binding sites in HIP1 uncover a general assembly role for endocytic accessory proteins. J. Biol. Chem. *276*, 46230–46236.

Mulholland, J., Preuss, D., Moon, A., Wong, A., Drubin, D., and Botstein, D. (1994). Ultrastructure of the yeast actin cytoskeleton and its association with the plasma membrane. J. Cell Biol. *125*, 381–391.

Mulholland, J., Wesp, A., Riezman, H., and Botstein, D. (1997). Yeast actin cytoskeleton mutants accumulate a new class of Golgi-derived secretary vesicle. Mol. Biol. Cell *8*, 1481–1499.

Munn, A.L., Stevenson, B.J., Geli, M.I., and Riezman, H. (1995). *end5*, *end6*, and *end7*: mutations that cause actin delocalization and block the internalization step of endocytosis in *S. cerevisiae*. Mol. Biol. Cell *6*, 1721–1742.

Nelson, K.K., Holmer, M., and Lemmon, S.K. (1996). *SCD5*, a suppressor of clathrin deficiency, encodes a novel protein with a late secretory function in yeast. Mol. Biol. Cell *7*, 245–260.

Nelson, K.K., and Lemmon, S.K. (1993). Suppressors of clathrin deficiency: overexpression of ubiquitin rescues lethal strains of clathrin-deficient *S. cerevisiae*. Mol. Cell. Biol. *13*, 521–532.

Novick, P., and Botstein, D. (1985). Phenotypic analysis of temperature-sensitive yeast actin mutants. Cell *40*, 405–416.

Payne, G.S., Baker, D., van Tuinen, E., and Schekman, R. (1988). Protein transport to the vacuole and receptor-mediated endocytosis by clathrin heavy chain-deficient yeast. J. Cell Biol. *106*, 1453–1461.

Pishvaee, B., Costaguta, G., Yeung, B.G., Ryazantsev, S., Greener, T., Greene, L.E., Eisenberg, E., McCaffery, J.M., and Payne, G.S. (2000). A yeast DNA J protein required for uncoating of clathrin-coated vesicles in vivo. Nat. Cell Biol. *2*, 958–963.

Pringle, J.R. (1991). Staining of bud scars and other cell wall chitin with calcofluor. Methods Enzymol. *194*, 732–735.

Pringle, J.R., Adams, A.E., Drubin, D.G., and Haarer, B.K. (1991). Immunofluorescence methods for yeast. Methods Enzymol. *194*, 565–602.

Pruyne, D., and Bretscher, A. (2000a). Polarization of cell growth in yeast. J. Cell Sci. *113*, 571–585.

Pruyne, D., and Bretscher, A. (2000b). Polarization of cell growth in yeast. I. Establishment and maintenance of polarity states. J. Cell Sci. *113*, 365–375.

Qualmann, B., Kessels, M.M., and Kelly, R.B. (2000). Molecular links between endocytosis and the actin cytoskeleton. J. Cell Biol. *150*, F111–F116.

Ramjaun, A.R., and McPherson, P.S. (1998). Multiple amphiphysin II splice variants display differential clathrin binding: identification of two distinct clathrin-binding sites. J. Neurochem. *70*, 2369–2376.

Raths, S., Rohrer, J., Crausaz, F., and Riezman, H. (1993). *end3* and *end4*: two mutants defective in receptor-mediated and fluid-phase endocytosis in *S. cerevisiae*. J. Cell Biol. *120*, 55–65.

Schaerer-Brodbeck, C., and Riezman, H. (2000). Functional interactions between the p35 subunit of the Arp2/3 complex and calmodulin in yeast. Mol. Biol. Cell *11*, 1113–1127.

Seeger, M., and Payne, G.S. (1992a). A role for clathrin in the sorting of vacuolar proteins in the Golgi complex of yeast. EMBO J. *11*, 2811–2818.

Seeger, M., and Payne, G.S. (1992b). Selective and immediate effects of clathrin heavy chain mutations on Golgi membrane protein retention in *S. cerevisiae*. J. Cell Biol. *118*, 531–540.

Seki, N., Muramatsu, M., Sugano, S., Suzuki, Y., Nakagawara, A., Ohhira, M., Hayashi, A., Hori, T., and Saito, T. (1998). Cloning, expression analysis, and chromosomal localization of HIP1R, an

isolog of huntingtin interacting protein (HIP1). J. Hum. Genet. *43*, 268–271.

Sikorski, R.S., and Hieter, P. (1989). A system of shuttle vectors and yeast host strains designed for efficient manipulation of DNA in *S. cerevisiae*. Genetics *122*, 19–27.

Sivadon, P., Bauer, F., Aigle, M., and Crouzet, M. (1995). Actin cytoskeleton and budding pattern are altered in the yeast *rvs161* mutant: the Rvs161 protein shares common domains with the brain protein amphiphysin. Mol. Gen. Genet. *246*, 485–495.

Slepnev, V.I., Ochoa, G.C., Butler, M.H., and DeCamilli, P. (2000). Tandem arrangement of the clathrin and AP-2 binding domains in amphiphysin 1 and disruption of clathrin coat function by amphiphysin fragments comprising these sites. J. Biol. Chem. *275*, 17583–17589.

Stark, M.J.R. (1996). Yeast protein serine/threonine phosphatases: multiple roles and diverse regulation. Yeast *12*, 1647–1675.

Tan, P.K., Davis, N.G., Sprague, G.F., and Payne, G.S. (1993). Clathrin facilitates the internalization of seven transmembrane segment receptors for mating pheromones in yeast. J. Cell Biol. *123*, 1707–1716.

Tang, H.Y., and Cai, M. (1996). The EH-domain-containing protein Pan1 is required for normal organization of the actin cytoskeleton in *S. cerevisiae*. Mol. Cell. Biol. *16*, 4897–4914.

Tang, H.Y., Munn, A., and Cai, M. (1997). EH domain proteins Pan1p and End3p are components of a complex that plays a dual role in organization of the cortical actin cytoskeleton and endocytosis in *S. cerevisiae*. Mol. Cell. Biol. *17*, 4294–4304.

Tang, H.Y., Xu, J., and Cai, M. (2000). Pan1p, End3p, and S1a1p, three yeast proteins required for normal cortical actin cytoskeleton organization, associate with each other and play essential roles in cell wall morphogenesis. Mol. Cell. Biol. *20*, 12–25.

Traub, L.M., Downs, M.A., Westrich, J.L., and Fremont, D.H. (1999). Crystal structure of the alpha appendage of AP-2 reveals a recruitment platform for clathrin-coat assembly. Proc. Natl. Acad. Sci. USA *96*, 8907–8912.

Tu, J.L., Song, W.J., and Carlson, M. (1996). Protein phosphatase type 1 interacts with proteins required for meiosis and other cellular processes in *S. cerevisiae*. Mol. Cell. Biol. *16*, 4199–4206.

Uetz, P., *et al.* (2000). A comprehensive analysis of protein-protein interactions in *S. cerevisiae*. Nature *403*, 623–627.

Valdivia, R.H., Baggott, D., Chuang, J.S., and Schekman, R.W. (2002). The yeast clathrin adaptor protein complex 1 is required for the efficient retention of a subset of late Golgi membrane proteins. Dev. Cell. *2*, 283–294.

Venturi, G.M., Bloecher, A., Williams-Hart, T., and Tatchell, K. (2000). Genetic interactions between *GLC7*, *PPZ1* and *PPZ2* in *S. cerevisiae*. Genetics *155*, 69–83.

Vojtek, A., Haarer, B., Field, J., Gerst, J., Pollard, T.D., Brown, S., and Wigler, M. (1991). Evidence for a functional link between profilin and CAP in the yeast *S. cerevisiae*. Cell *66*, 497–505.

Wach, A. (1996). PCR-synthesis of marker cassettes with long flanking homology regions for gene disruptions in *S. cerevisiae*. Yeast *12*, 259–265.

Waelter, S., *et al.* (2001). The huntingtin interacting protein HIP1 is a clathrin- and alpha-adaptin-binding protein involved in receptor-mediated endocytosis. Hum. Mol. Genet. *10*, 1807–1817.

Wanker, E.E., Rovira, C., Scherzinger, E., Hasenbank, R., Walter, S., Tait, D., Colicelli, J., and Lehrach, H. (1997). HIP-I: a huntingtin interacting protein isolated by the yeast two-hybrid system. Hum. Mol. Genet. *6*, 487–495.

Wendland, B., and Emr, S.D. (1998). Pan1p, yeast Eps15, functions as a multivalent adaptor that coordinates protein-protein interactions essential for endocytosis. J. Cell Biol. *141*, 71–84.

Wendland, B., McCaffery, J.M., Xiao, Q., and Emr, S.D. (1996). A novel fluorescence-activated cell sorter-based screen for yeast endocytosis mutants identifies a yeast homologue of mammalian eps15. J. Cell Biol. *135*, 1485–1500.

Wendland, B., Steece, K.E., and Emr, S.D. (1999). Yeast epsins contain an essential N-terminal ENTH domain, bind clathrin and are required for endocytosis. EMBO J. *18*, 4383–4393.

Wesp, A., Hicke, L., Palecek, J., Lombardi, R., Aust, T., Munn, A.L., and Riezman, H. (1997). End4p/Sla2p interacts with actin-associated proteins for endocytosis in *S. cerevisiae*. Mol. Biol. Cell *8*, 2291–2306.

Yang, S., Ayscough, K.R., and Drubin, D.G. (1997). A role for the actin cytoskeleton of *S. cerevisiae* in bipolar bud-site selection. J. Cell Biol. *136*, 111–123.

Yang, S., Cope, M.J., and Drubin, D.G. (1999). Sla2p is associated with the yeast cortical actin cytoskeleton via redundant localization signals. Mol. Biol. Cell *10*, 2265–2283.

Zeng, G., and Cai, M. (1999). Regulation of the actin cytoskeleton organization in yeast by a novel serine/threonine kinase Prk1p. J. Cell Biol. *144*, 71–82.

Zeng, G., Yu, X., and Cai, M. (2001). Regulation of yeast actin cytoskeleton-regulatory complex Pan1p/Sla1p/End3p by serine/threonine kinase Prk1p. Mol. Biol. Cell *12*, 3759–3772.